Signal processing techniques for characterizing nonlinear processes in turbulent plasmas

Gérard BONHOMME

Laboratoire de Physique des Milieux Ionisés et Applications,
CNRS-UMR 7040, Université Henri Poincaré, Nancy

Gerard.Bonhomme@lpmi.uhp-nancy.fr

Thanks to: F. Brochard, E. Gravier, A. Scipioni, P. Rischette, *LPMIA, Nancy*

T. Windisch, O. Grulke, T. Klinger, *IPP-Greifswald*

J. Gunn, N. Fedorczak, P. Devynck, *DRFC-Association EURATOM-CEA Cadarache*

Outline

- Introduction
  - What is measured and what can be inferred
  - Drawbacks of the Fourier based methods for signals from turbulence
- Wavelet based methods
  - Principle of the Wavelet Transform
  - Continuous vs Discrete Wavelet Transforms
  - Applications: time-frequency analysis, self-similarity properties,
- The Hilbert-Huang transform
  - The Empirical Mode Decomposition
  - Applications
- Nonlinear wave-wave coupling
- Conclusions

Turbulence and transport in the Scrape-off-Layer of Tokamaks

- Essential role played by intermittent and large scale structures ("blobs") in the cross-field energy and particle transport to the wall in the far Scrape-Off-Layer (SOL)
- From many experimental studies carried out in several machines (toroidal : Tore-Supra, W-7AS, Alcator-C, NSTX, D-IIID, … and linear machines as well →

  - radially propagating "blobs" are responsible for ~50% of the transport

  - Study of statistical properties → signature of intermittency and "blobs" and of self-similarity (Hurst parameter ⇒ long-range correlations, SOC models?, …)
- Open questions:

  - Origin and formation of the "blobs" (core plasma, relation with ELMs?, near the separatrix, inverse cascade process?), propagation velocity, time and size scales,

  → need for Diagnostics (probes arrays, imaging, …), signal processing methods, comparison with numerical simulations, …

Time-series analysis (probe data)

Data in the form of time series are collected from a turbulent process ⇒

How can we extract information from these time series

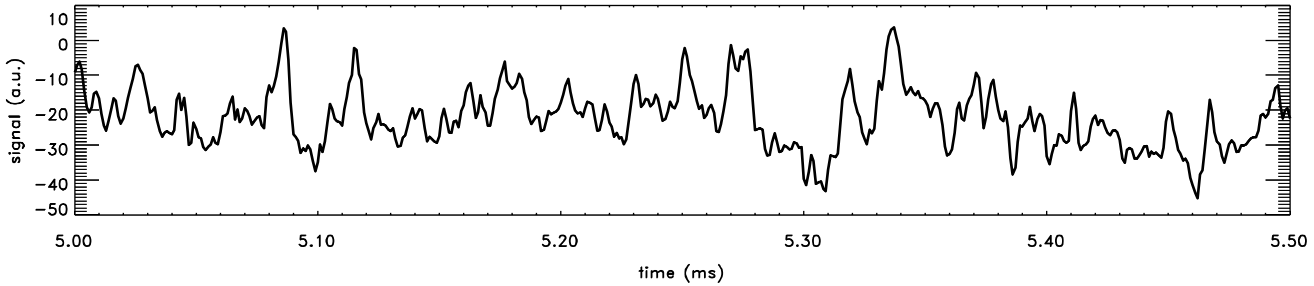

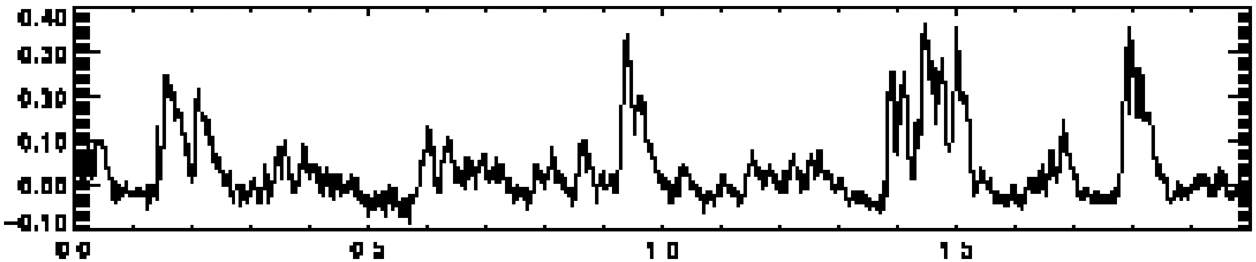

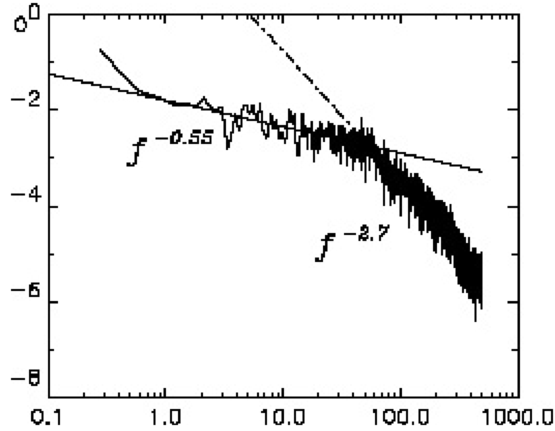

Experimental data from tokamaks

Intermittency, non linearity ⇒

"Classical" Methods =

- Statistical Analysis → stationary stochastic processes
- Fourier Methods = projection on an orthogonal basis, but with infinite support ⇒ Limitations

are inadequate

Tore-Supra (Shot #35000)

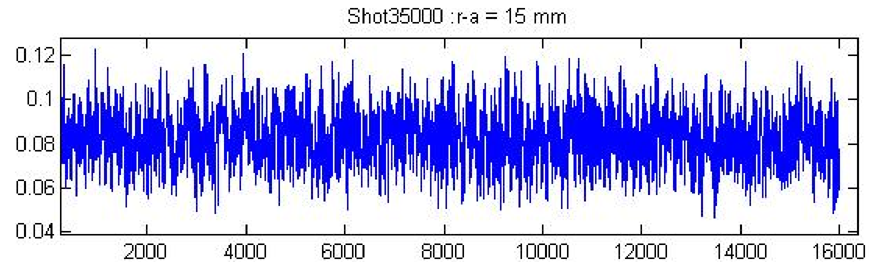

2B Isat,

x_m = 0,0822

σ = 0,0118

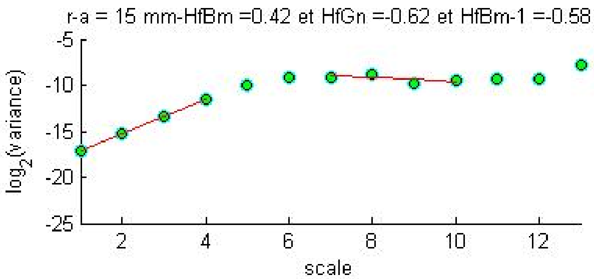

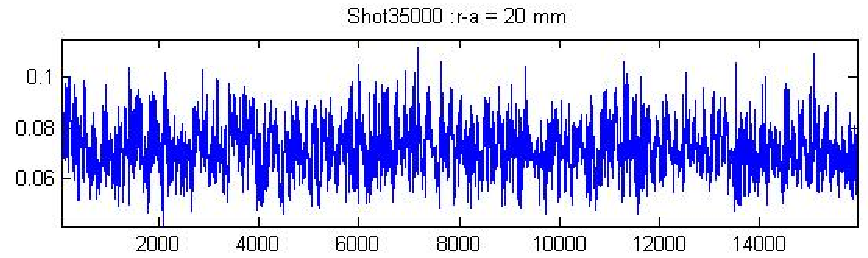

2B Isat,

x_m = 0,072

σ = 0,0094

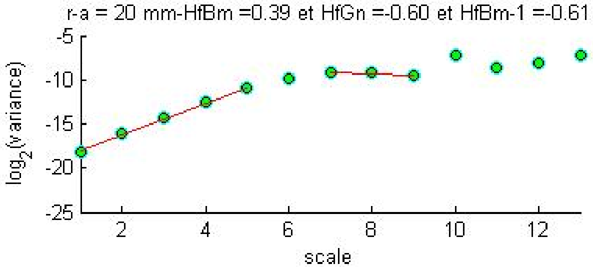

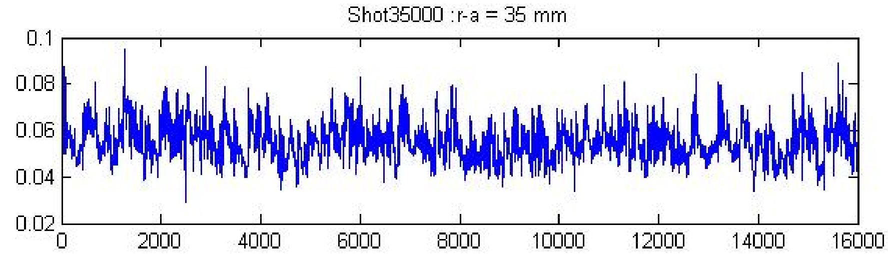

2B Isat,

x_m = 0,0551

σ = 0,0076

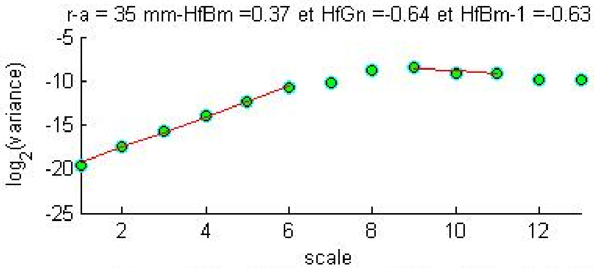

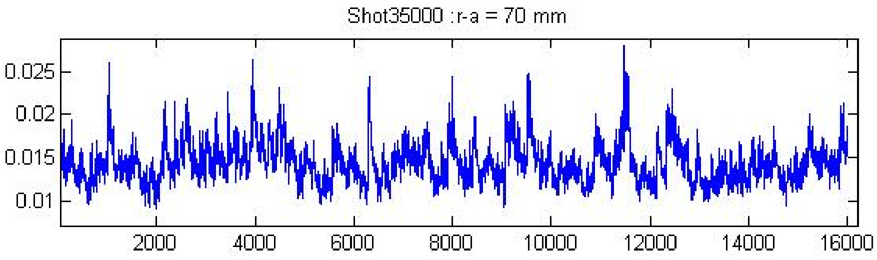

2B Isat,

x_m = 0,0144

σ = 0,0023

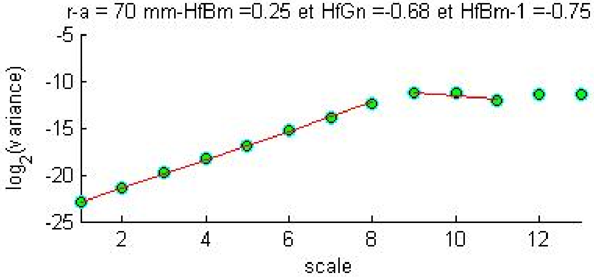

Tore-Supra Shot #35000

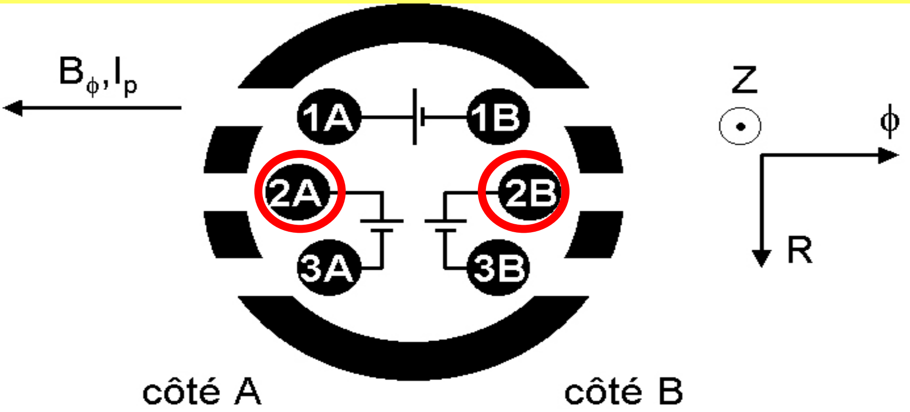

Analyzed signals: Isat_2A et Isat_2B
for *r* = 15, 20, 35, 70 mm (distance to LCFS)

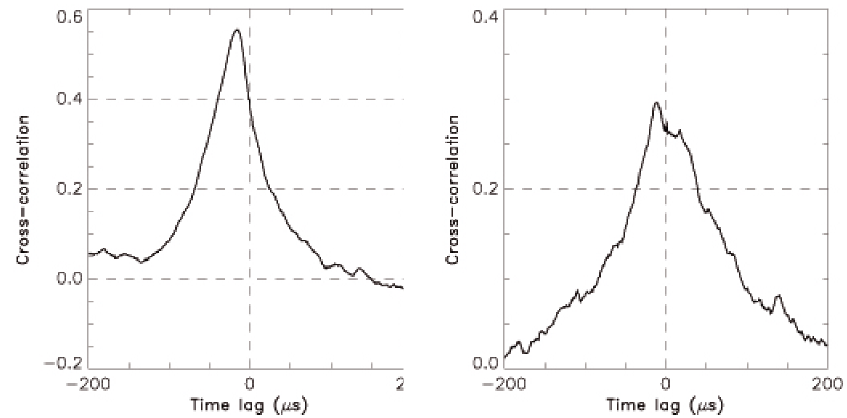

I1A-I2A

I2A-I3A

Cross-correlations r = 15 mm

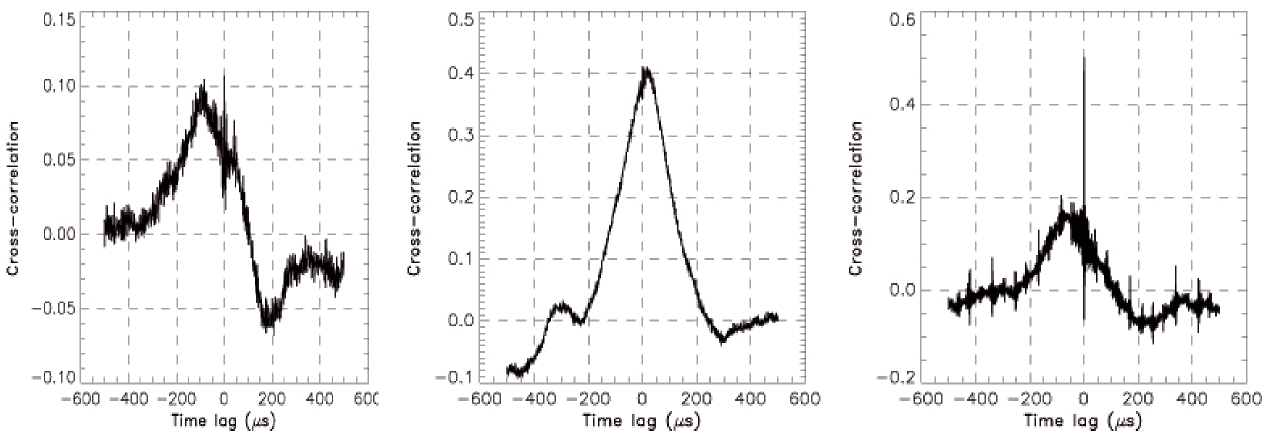

I1A-I2A

I2A-I3A

I1A-I3A

Cross-correlations r = 70 mm

Non Gaussian PDF related to intermittency

Tore-Supra Shot #35000

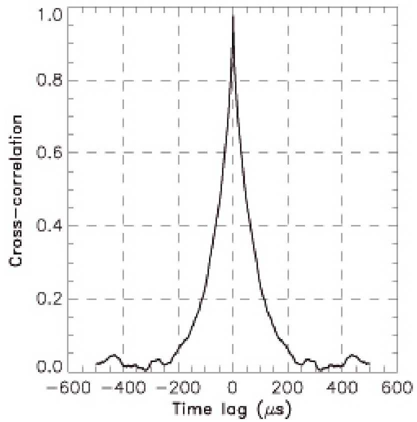

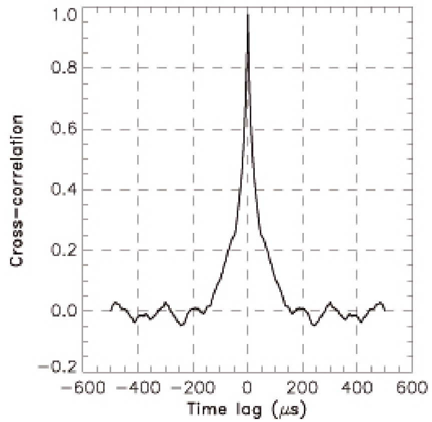

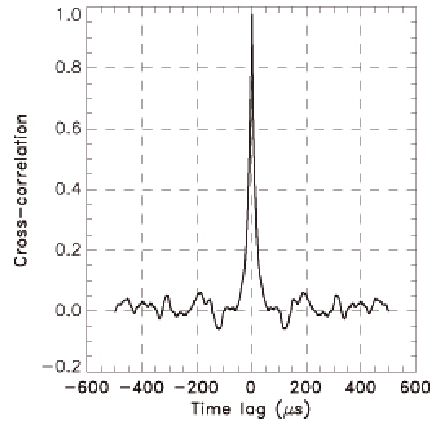

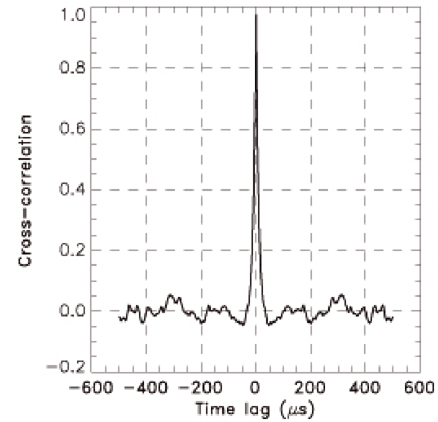

2B Isat, *r* = 70 mm

2B Isat, *r* = 35 mm

2B Isat, *r* = 20 mm

2B Isat, *r* = 15 mm

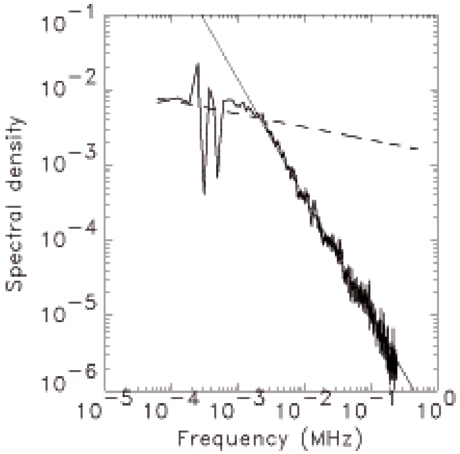

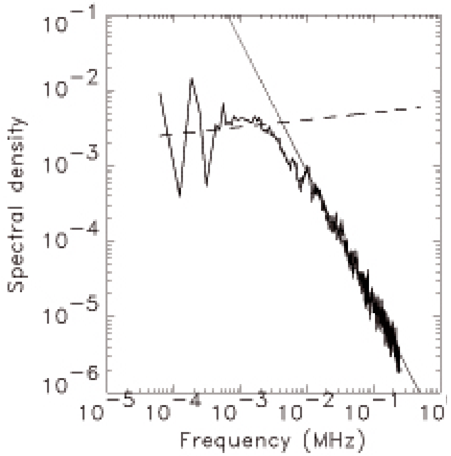

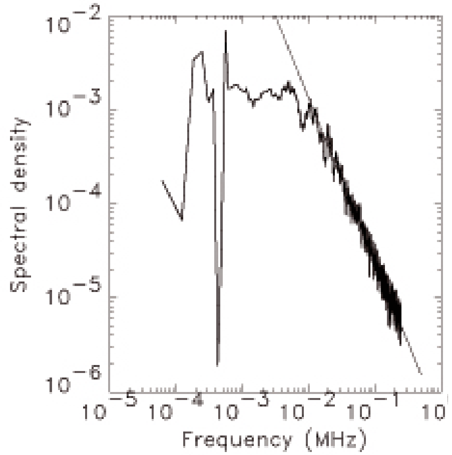

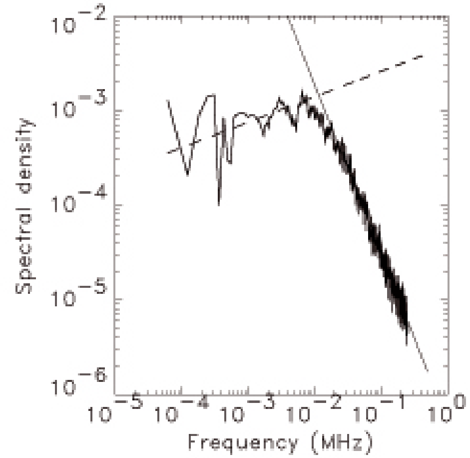

Autocorrelations and Fourier spectra

Tore-Supra Shot #35000

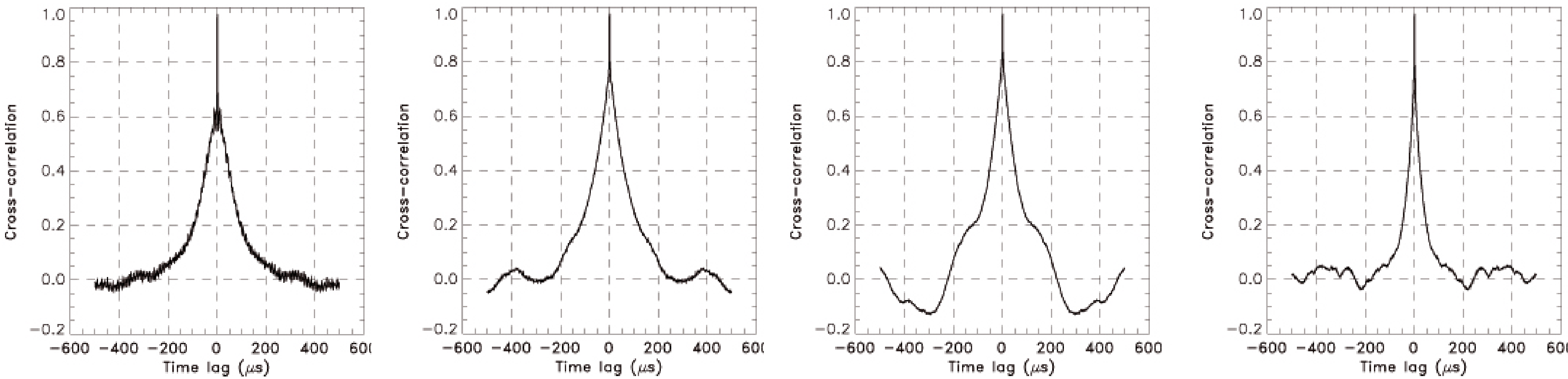

2A Isat, r = 70 mm | 2A Isat, r = 35 mm | 2A Isat, r = 20 mm | 2A Isat, r = 15 mm

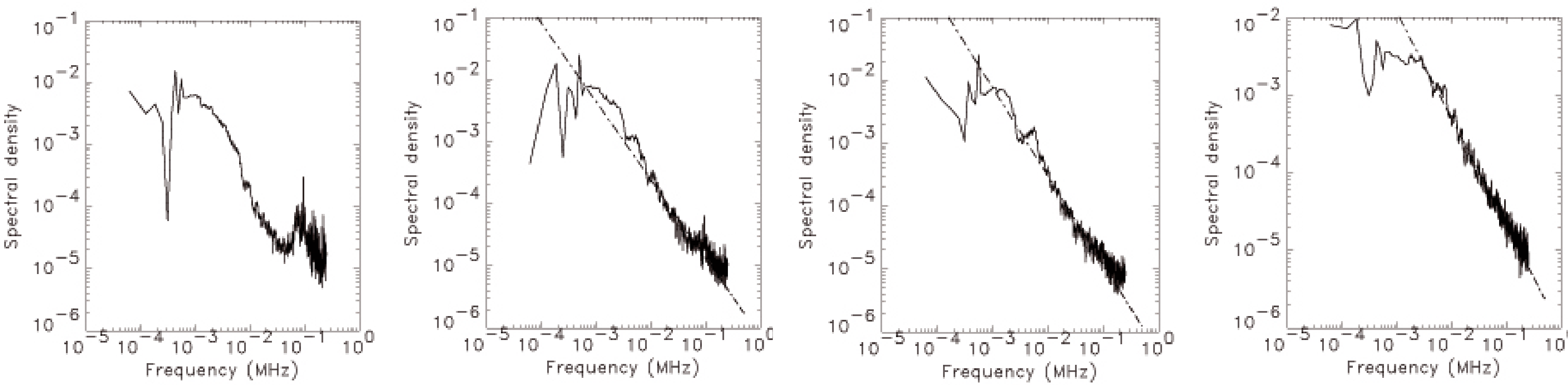

Autocorrelations and Fourier spectra

Drawbacks of Fourier methods

Fourier transform definition: $$F(\omega)=\int_{-\infty}^{+\infty} f(t)e^{-i\omega t}dt \quad \Leftrightarrow \quad f(t)=\frac{1}{2\pi}\int_{-\infty}^{+\infty} F(\omega)e^{+i\omega t}d\omega$$

$\Rightarrow$ *F* (ω) complex $\Rightarrow$ Information on time localisation contained in the phase

$\Rightarrow$ difficult access

- Example 1 $\rightarrow$ A musician playing either successively two $\neq$ notes, or simultaneously these two notes $\Rightarrow$ same amplitude spectra

$$S_{ff}(\omega)=\left|F(\omega)\right|^2$$

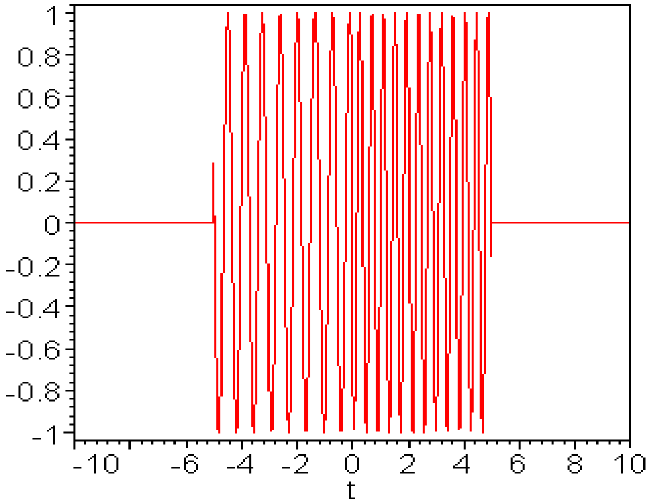

$$\begin{cases}\sin\omega_0(t-\tau) & -5<t<0\\ \sin 1.5\omega_0(t-\tau) & 0<t<5\end{cases}$$

with $\tau = 1.$; ω_0 =10

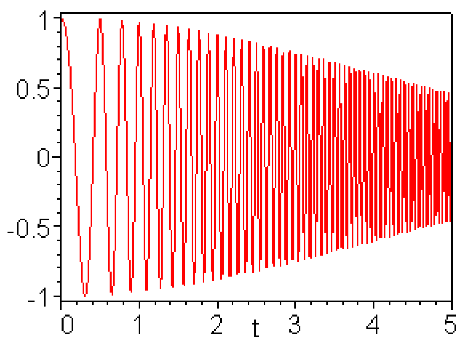

$$e^{-\pi t^2/\delta^2}\cos 2\pi(f_0 t+\beta t^2)$$

with δ=10 ; β=2. ; f_0=1

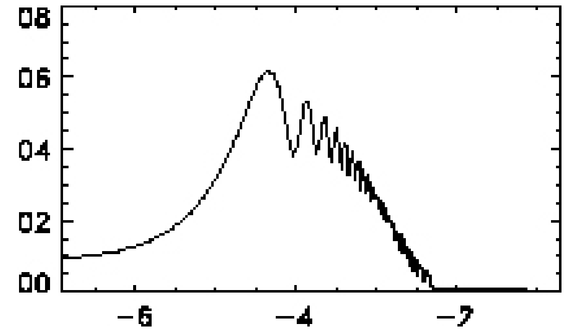

Spectral density

chirp

Solution: Wavelets?

- Short-time (or windowed) Fourier transform

$\rightarrow$ (DFT of sub-series) $\Rightarrow$ Pb : frequency resolution $\Delta\nu = 1/T$

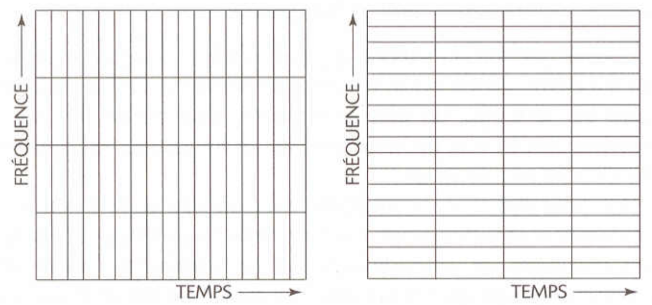

the time resolution is the same at all frequencies

- Wavelet transform = generalization of the Fourier analysis

$\rightarrow$ change for an other analysis function giving a time resolution depending on the frequency

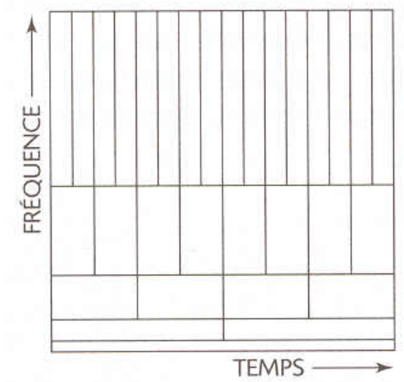

$\Rightarrow$ find an orthogonal basis localised in time <u>and</u> frequency

Intermittency between two modes

Ionization waves in a glow discharge (I = 3 mA)

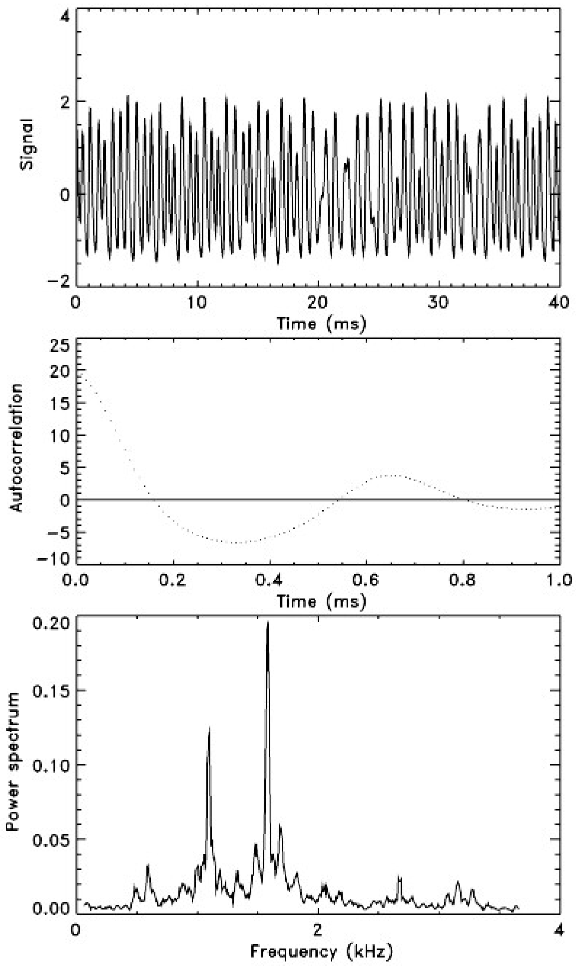

f_1 = 1.05 kHz, f_2 = 1.55 kHz

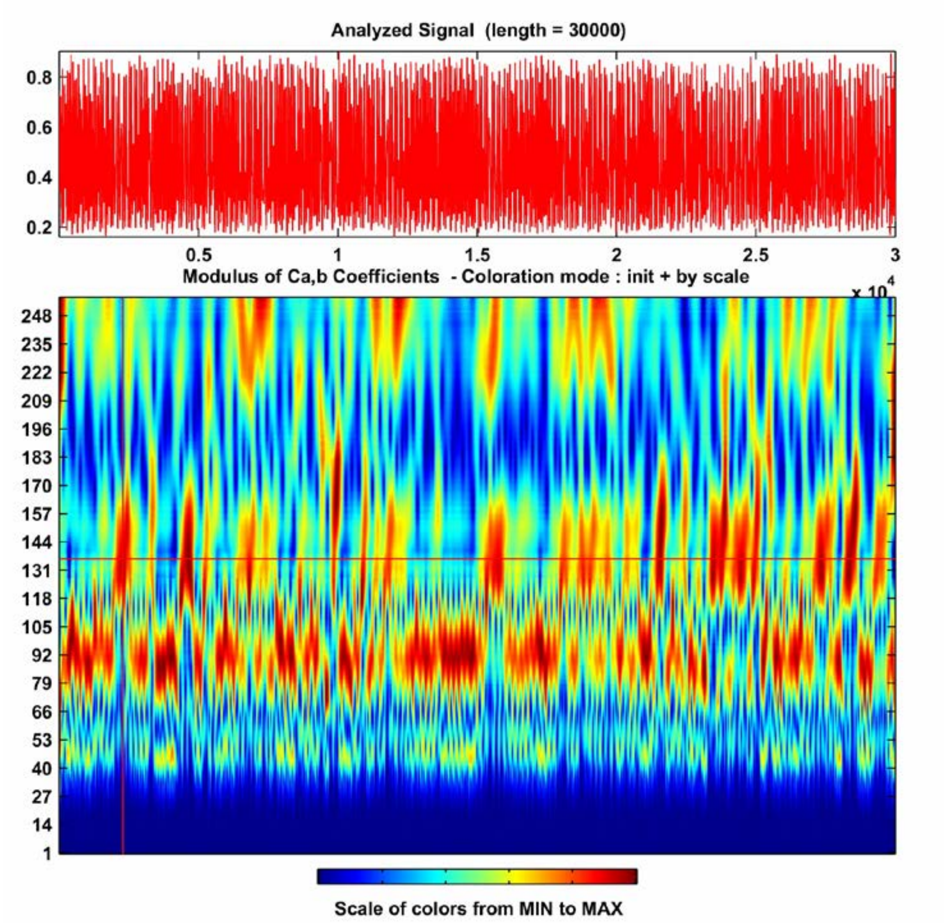

Time-frequency representation (Morlet)

Periodic pulling

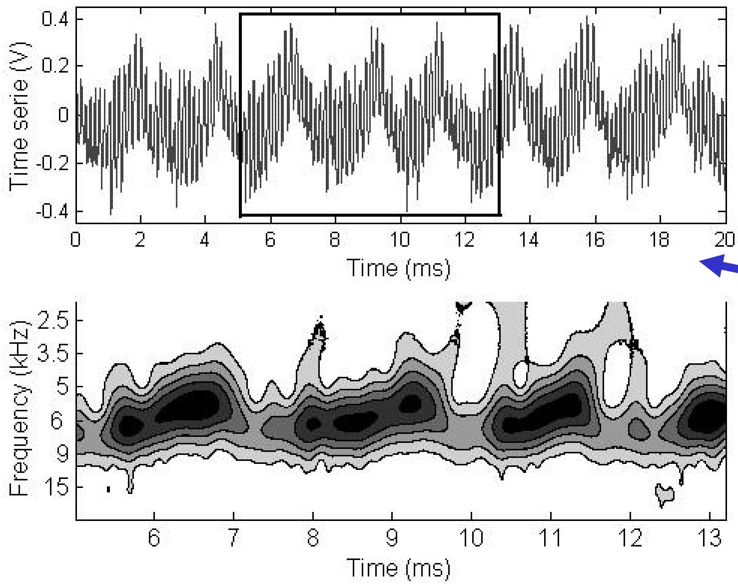

K-H instability

U_d=50 volts

Time series "y5a02" at r = 4 cm (in the shear layer)

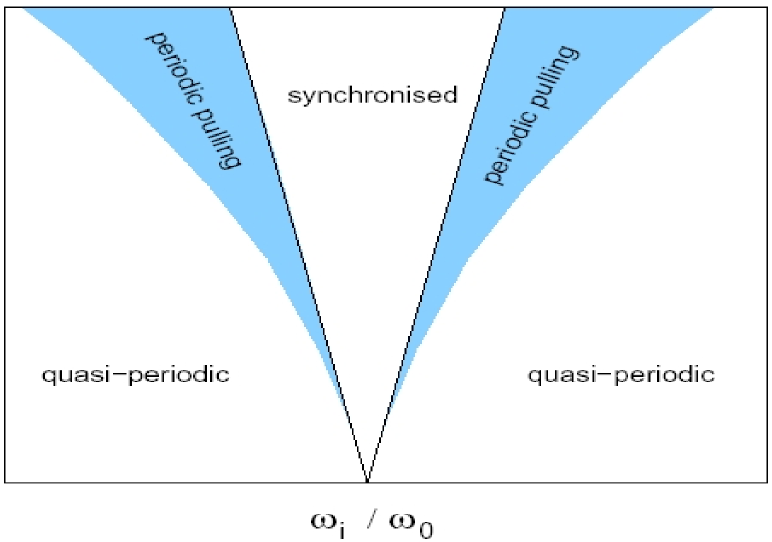

A=1., ε =1.

ω_1 = 1.2

"VdP1.0-1.2"

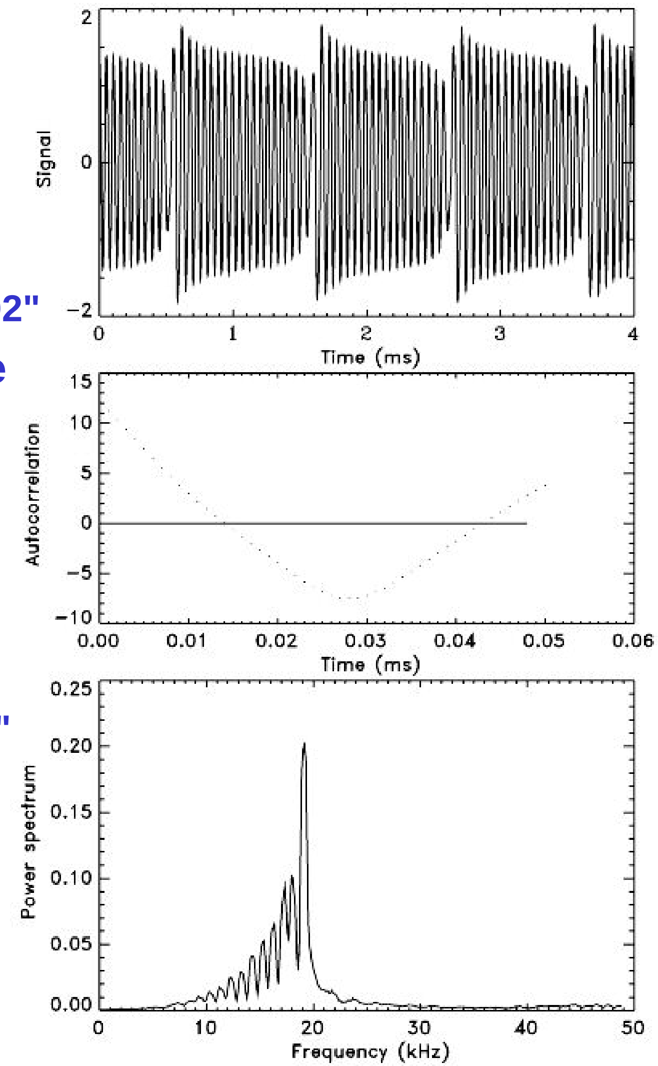

$$\ddot{x}+\varepsilon\left(x^2-1\right)\omega_0\,\dot{x}+\omega_0^2\,x=A\cos\left(\omega_1 t\right)$$

a simple model: the forced van der Pol oscillator

Wavelet Analysis

- Principle of the wavelet transform:

replace the sine waves of the Fourier decomposition by orthogonal basis functions localised in time and frequency

- Aim : Decomposition of a signal into components (small waves, i.e. wavelets) corresponding to :

  ≠ scales or levels (i.e., frequencies) and

  ≠ localisations for each of these scales

$$\varphi_{T,t_0}(t) = \varphi\left(\frac{t-t_0}{T}\right)$$

$$W_\varphi^f(T,t_0) = \frac{1}{\sqrt{T}} \int_{-\infty}^{+\infty} f(t)\varphi_{T,t_0}^*(t)dt$$

→ Two different approaches :

- Continuous Wavelet Transform (e.g. Morlet) → time-frequency analysis
- Discrete Wavelet Transform → orthogonal decomposition (filtering)

The Continuous Wavelet Transform

Principle : mother-wavelet φ(t) ⇒ $\varphi_{T,t_0}(t) = \varphi\left(\frac{t-t_0}{T}\right)$ Translation + dilatation

⇒ Wavelet Transform $W_\varphi^f(T,t_0) = \frac{1}{\sqrt{T}} \int_{-\infty}^{+\infty} f(t)\varphi_{T,t_0}^*(t)dt$ $\frac{1}{\sqrt{T}}$ → normalisation

Pb : find a "good " mother-wavelet

- compact support
- orthogonal basis in L^2(R)

⇒ Necessary conditions (admissibility) :

- $0 < c_\varphi = \int_{-\infty}^{+\infty} \frac{|\varphi(t)|^2}{t} dt < \infty \quad \Rightarrow \quad f(t) = \frac{1}{c_\varphi} \int_0^{+\infty} dT \int_{-\infty}^{+\infty} W_\varphi^f(T,t_0)\sqrt{T}\varphi_{T,t_0}^*\left(\frac{t-t_0}{T}\right)dt_0$ (reconstruction)
- $\int_{-\infty}^{+\infty} |\varphi(t)| dt < \infty \quad \rightarrow \quad \text{localisation}$

Parseval's theorem → $\int_{-\infty}^{+\infty} |f(t)|^2 dt = \frac{1}{c_\varphi} \int_0^{+\infty} dT \int_{-\infty}^{+\infty} |W_\varphi^f(T,t_0)|^2 dt_0$

⇒ Morlet wavelets $\varphi(t) = Ce^{-i2\pi dt}(e^{-t^2/2} - c_0 e^{-t^2})$ with $c_0 = \sqrt{2}e^{-\pi^2 d^2}$

$\Delta t \Delta\omega = \pi$ with: Time resolution $\Delta t = 2Td$ Frequency resolution $\Delta\omega \approx \omega/4d$ (with $\omega = \frac{2\pi}{T}$)

Time-frequency analysis

- pulse

$$e^{-\alpha(t-\tau)^2}\cos\omega_0 t$$

$\alpha = 0.1$; $\tau = 1.$; $\omega_0 = 10$

- *chirp*

$$e^{-\pi t^2/\delta^2}\cos 2\pi(f_0 t + \beta t^2)$$

$\delta = 10$;

$\beta = 0.5$; $f_0 = 0.5$

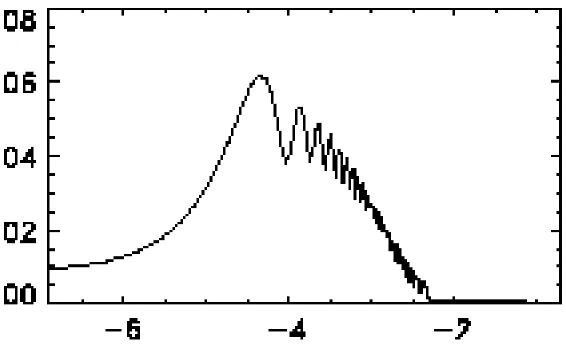

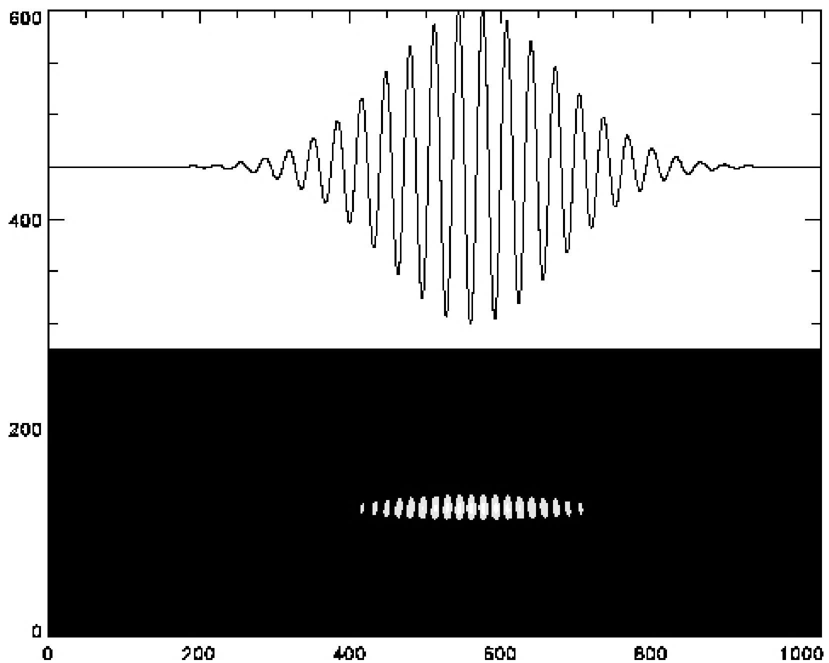

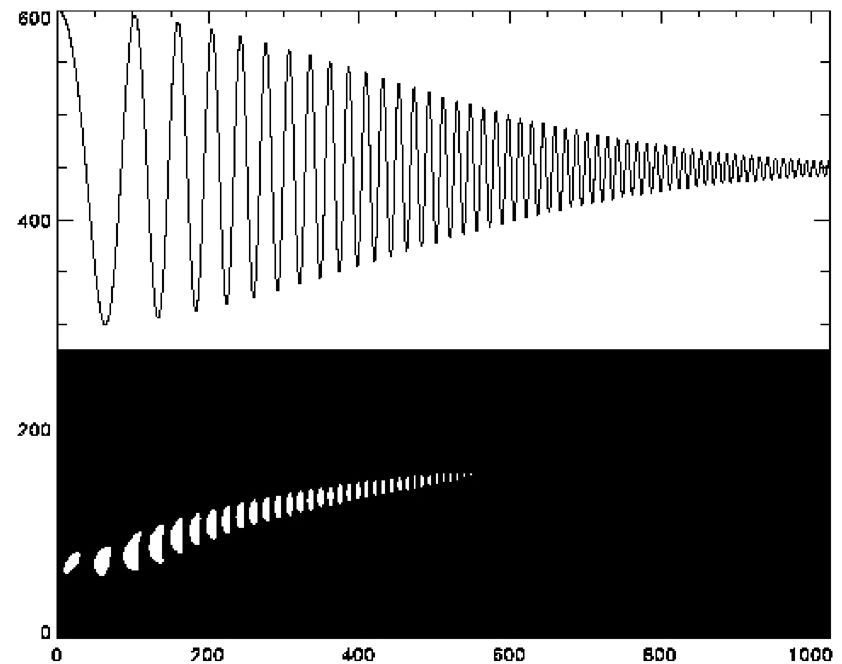

The Morlet Wavelet

φ

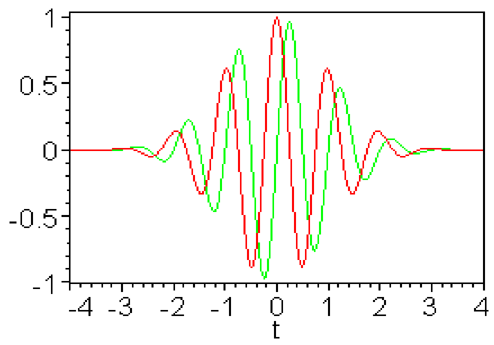

$d = 1 \Rightarrow$

Mother-wavelet

k=2π, t_0=0, T=1

Φ

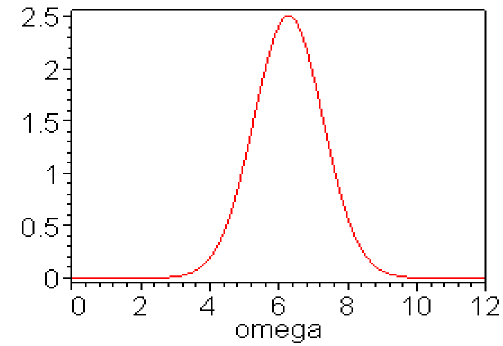

$$\varphi_{T,t_0}(t) = \frac{1}{\sqrt{T}} \exp\left[-\frac{1}{2}\left(\frac{t-t_0}{T}\right)^2 + ik\frac{t-t_0}{T} \right]$$

$$\Phi_{T,t_0}(\omega) = \sqrt{T}\sqrt{2\pi}\exp\left[-i\omega t_0 + k\omega T - \frac{1}{2}\left(k^2 + \omega^2 T^2\right) \right]$$

Maximum at $\omega T = k$

Morlet transform:

$$W_\varphi^f(T,t_0) = \frac{1}{\sqrt{T}} \int_{-\infty}^{+\infty} f(t)\varphi^*_{T,t_0}(t)dt = \frac{1}{\sqrt{T}} \int_{-\infty}^{+\infty} f(t)\frac{1}{\sqrt{T}} \exp\left[-\frac{1}{2}\left(\frac{t-t_0}{T}\right)^2 - ik\frac{t-t_0}{T} \right] dt$$

convolution product $f_* \varphi_T \Rightarrow$

$$W_\varphi^f(T,t_0) = \frac{1}{\sqrt{T}} TF^{-1}\left[TF(f)TF(\varphi_T)\right]$$

with

$$FT(\varphi) = \Phi_T(\omega) = \sqrt{T}\sqrt{2\pi}\exp\left[k\omega T - \frac{1}{2}\left(k^2 + \omega^2 T^2\right) \right]$$

The Discrete Wavelet Transform

Drawbacks of the continuous wavelet transform : redondancy, CPU time, admissibility conditions non completely fullfilled (Morlet)

Solution ? Discrete Wavelets (similar to the DFT)

- Octave scaling →

  $T_j = 2^j$ et $t_{0\,j,k} = k/2^j$

$$W_{m,k}(t) = 2^{m/2} W(2^m t - k)$$

- orthogonality $$\langle W_{m,k}, W_{n,l} \rangle = \delta_{mn}\delta_{kl}$$

with $$\langle h, g \rangle = \int_{-\infty}^{+\infty} h^*(t) g(t) dt$$

There are 2^m base functions at the *m* level

$$\Rightarrow \quad X_k^m = \int_{-\infty}^{\infty} x(t) W_{m,k}^*(t) dt \quad \rightarrow \quad x_m(t) = \sum_k X_m^k W_{m,k}(t)$$

- reconstruction $$x(t) = \sum_{m,k} X_m^k W_{m,k}(t)$$

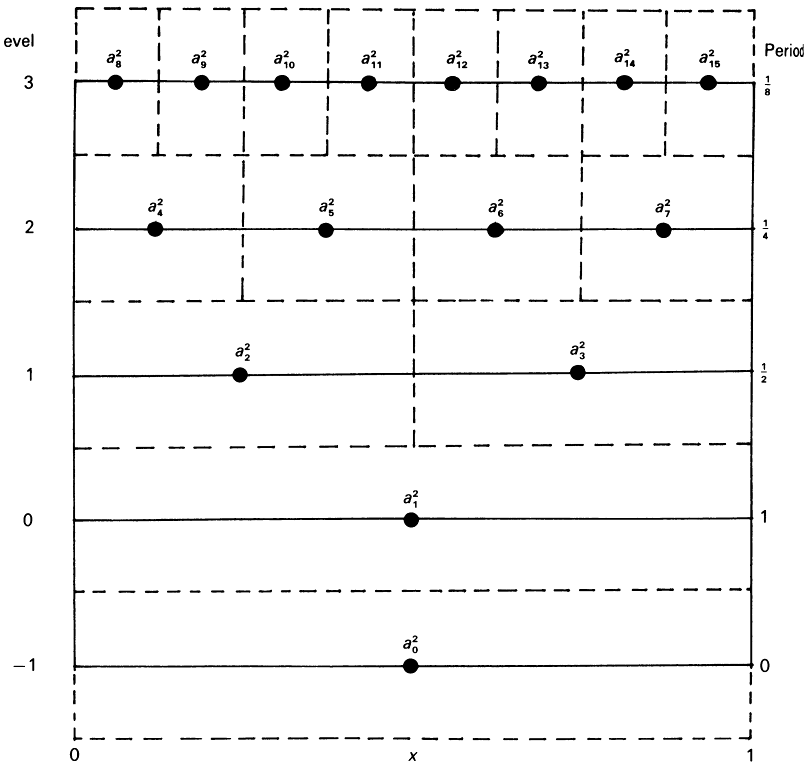

Fig. 17.18 Grid base for plotting wavelet amplitudes (squared) in order to ensure that the volume they enclose is equal to the mean-square value of $f(x)$

from Newland [1]

Wavelet construction: Daubechies wavelet

- Haar

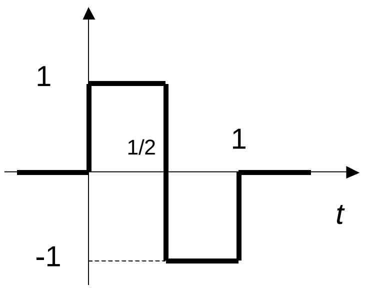

lack of regularity $\Rightarrow$

- Daubechies wavelets

$$W(t) = \sum_{k=0}^{2r-1} (-1)^k c_k \Phi(2t + k - 2r + 1)$$

- must be determined by recurrence from a scaling function $\Phi(t)$

(Meyer, 1993)

$$\Phi(t) = \frac{1}{\sqrt{2}} \sum_{k=0}^{2r-1} c_k \Phi(2t - k)$$

- they are completely defined by the coefficients c_k

2r+1 conditions must be satisfied:

$$\begin{cases} \sum_{k=0}^{2r-1} c_k = 2 \,, \sum_{k=0}^{2r-1} c_k^2 = 2 \\ \sum_{k=0}^{2r-1} (-1)^k k^m c_k = 0 \quad \text{for } m = 0, \ldots, r-1 \\ \sum_{k=0}^{2r-1} c_k c_{k+2m} = 0 \quad \text{for } m \neq, m = 1, 2, \ldots, r-1 \end{cases}$$

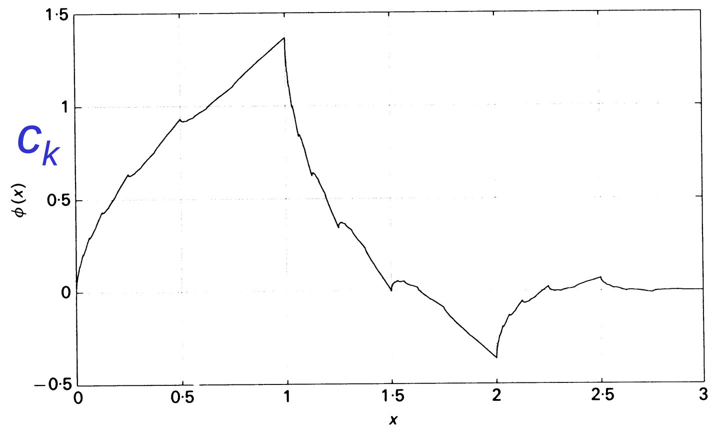

Fig. 17.5 Scaling function for the D4 wavelet calculated for $3 \times 2^{12} = 12\,288$ points using the recursive method described in problem 17.2

$\Phi(t)$ for r=2 (from Newland [1])

Mallat tree (pyramid algorithm)

- **Solutions :**

• Haar (r=1) → $c_0 = c_1 = 1$

• Daubechies $D4$ (r=2) →

$$\begin{cases} c_0 = \frac{1}{4}(1+\sqrt{3}),\ c_1 = \frac{1}{4}(3+\sqrt{3}) \\ c_2 = \frac{1}{4}(3-\sqrt{3}),\ c_3 = \frac{1}{4}(1-\sqrt{3}) \end{cases}$$

• $r > 3$, (numerical computation) → discrete transform (computed by using the Mallat algorithm) → analysis, and reconstruction formula → synthesis

$$f(t) = a_0\Phi(t) + a_1 W(t) + \begin{bmatrix} a_2 & a_3 \end{bmatrix} \begin{bmatrix} W(2t) \\ W(2t-1) \end{bmatrix} + \begin{bmatrix} a_4 & a_5 & a_6 & a_7 \end{bmatrix} \begin{bmatrix} W(4t) \\ W(4t-1) \\ W(4t-2) \\ W(4t-3) \end{bmatrix} + \cdots + a_{2^j+k} W(2^j t - k) + \cdots$$

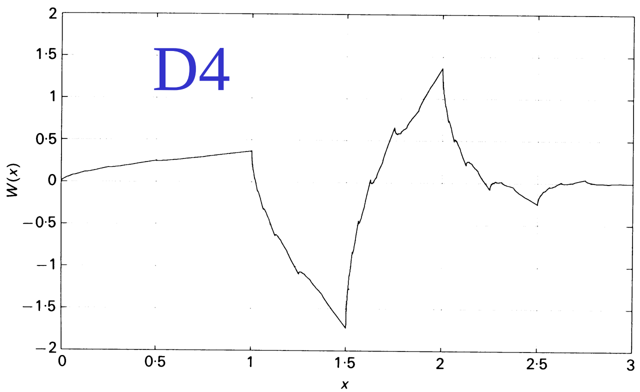

Fig. 17.6 D4 wavelet according to (17.5) from the scaling function in Fig. 17.5

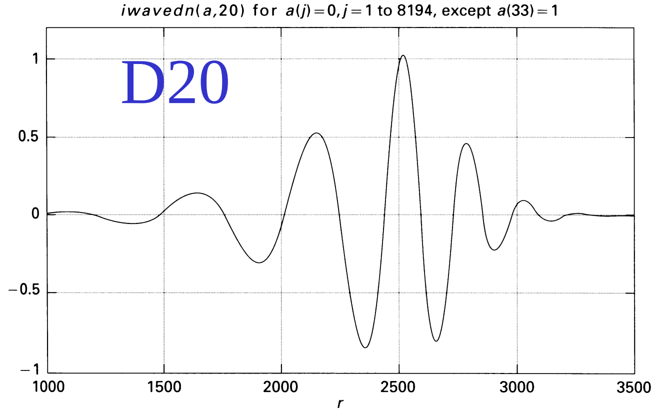

Fig. 17.13 Part of the D20 wavelet $W(16x)$ for a sequence length of 8192; the full wavelet occupies 19 intervals from integer 1 to 19(8192/32) = 4864

from Newland [1]

Practical considerations (1)

- The Continuous Wavelet Transform (Morlet):

FFT computation of $$W_\varphi^f(T,t_0) = FFT^{-1}\left[FFT(f)\exp(k\omega T - \frac{1}{2}k^2 - \frac{1}{2}\omega^2 T^2)\right]$$

⇓

Practically $f=\{f_n\}$ et $N=2^m$

⇓

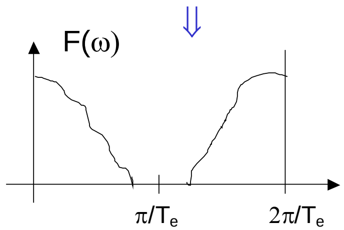

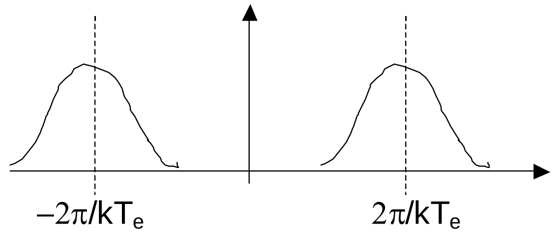

$$\frac{2}{NT_e} < \frac{4\pi}{kT} < \frac{1}{T_e} \quad \text{pour } k = 2\pi$$

⇒ Oversampling of $F(\omega)$ required

solution = zero padding of f_n (for $T=NT_e$ → $(N-1)N$ zeros)

See for example, D. Jordan et al, Rev.Sci.Instrum. 68 (1997) 1484-1494

Practical considerations (2)

• Discrete Wavelet Transform: $\rightarrow$ pyramid algorithm (no need for the $W(t)$)

example : $f=f(1{:}8) \xrightarrow{\frac{1}{2}L_3} f'(1{:}4) \xrightarrow{\frac{1}{2}H_2} f'(1{:}2) \xrightarrow{\frac{1}{2}H_1} f'(1)$

$\downarrow \frac{1}{2} H_3$ $\quad\downarrow \frac{1}{2} H_2$ $\quad\downarrow \frac{1}{2} H_1$ $\quad\downarrow$

$a[5{:}8]$ $\quad a[3{:}4]$ $\quad a(2)$ $\quad a(1)$

H_n et L_n are matrices build directly from the c_k coefficients (cf. Newland [1])

$$\mathbf{L_1} = \begin{bmatrix} c_0 + c_2 & c_1 + c_3 \end{bmatrix}$$

$$\mathbf{L_2} = \begin{bmatrix} c_0 & c_1 & c_2 & c_3 \\ c_2 & c_3 & c_0 & c_1 \end{bmatrix}$$

$$\mathbf{L_3} = \begin{bmatrix} c_0 & c_1 & c_2 & c_3 & & & & \\ & & c_0 & c_1 & c_2 & c_3 & & \\ & & & & c_0 & c_1 & c_2 & c_3 \\ c_2 & c_3 & & & & & c_0 & c_1 \end{bmatrix}$$

Low-pass filter

$$\mathbf{H_1} = \begin{bmatrix} -c_3 - c_1 & c_2 + c_0 \end{bmatrix}$$

$$\mathbf{H_2} = \begin{bmatrix} -c_3 & c_2 & -c_1 & c_0 \\ -c_1 & c_0 & -c_3 & c_2 \end{bmatrix}$$

$$\mathbf{H_3} = \begin{bmatrix} -c_3 & c_2 & -c_1 & c_0 & & & & \\ & & -c_3 & c_2 & -c_1 & c_0 & & \\ & & & & -c_3 & c_2 & -c_1 & c_0 \\ -c_1 & c_0 & & & & & -c_3 & c_2 \end{bmatrix}$$

High-pass filter

Times-series and self-similarity properties

Scale Invariance $\rightarrow$ self-similar stochastic process

- Definition and properties:
- Power spectrum $S_{xx}(\omega) = \dfrac{\sigma_x^2}{|\omega|^\gamma}$ γ characteristic exponent
- Algebraic decay of the autocorrelation function

$x(t) \equiv a^{-H} x(at)$ with H Hurst exponent, γ **=** 2*H* + *1*

$$\begin{cases} \langle x(t) \rangle \equiv a^{-H} \langle x(at) \rangle \\ \langle x(t_1) x(t_2) \rangle \equiv a^{-H} \langle x(at_1) x(at_2) \rangle \end{cases}$$

$\Rightarrow$ *x*(*t*) et *x*(*at*) have the same statistics

- constant correlation between past and future increments at all time:

$$C(t) = \langle (B_H(0) - B_H(-t))(B_H(t) - B_H(0)) \rangle / \langle B_H(t)^2 \rangle = 2^{2H-1} - 1$$

- Examples: * Gaussian white noise $\rightarrow$ **(γ = 0)** ***H* = - *1/2***

  * Fractional Brownian motion (fBm) **1< γ<3** $\rightarrow$ **0 <*H* < *1***

  Random walk (H = 0.5), 1/f processes, S.O.C.

R/S analysis and the Hurst exponent (1)

The rescaled ranged statistics (R/S) method was proposed to evaluate the Hurst exponent (*H*) to determine long time dependencies in various signals.

From a time series *X* of length *N*, sub-blocks of length *n* : $X = \{X_t : t = 1,2,\dots n\}$

are build to compute (with $W_k = X_1 + X_2 + \cdots + X_k - k\overline{X}(n),$):

$$\frac{R(n)}{S(n)} = \frac{\max(0, W_1, W_2, \cdots, W_n) - \min(0, W_1, W_2, \cdots, W_n)}{\sqrt{S^2(n)}}$$

$\overline{X}(n)$ mean

$S^2(n)$ variance

X = increments (fGn) of self-affine data (e.g., fractional Brownian motion)

→ $R/S \sim c\, n^H$

For uncorrelated data → $H = 0.5$ (*X* = time-series of a white noise)

If $H < 0.5$ → *antipersistence*

If $H > 0.5$ → *persistence*

R/S analysis and the Hurst exponent (2)

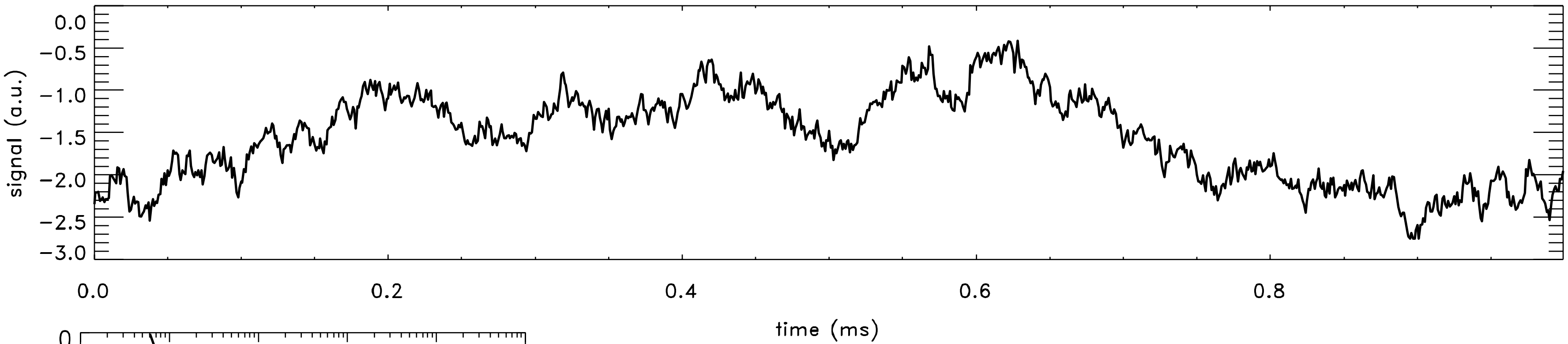

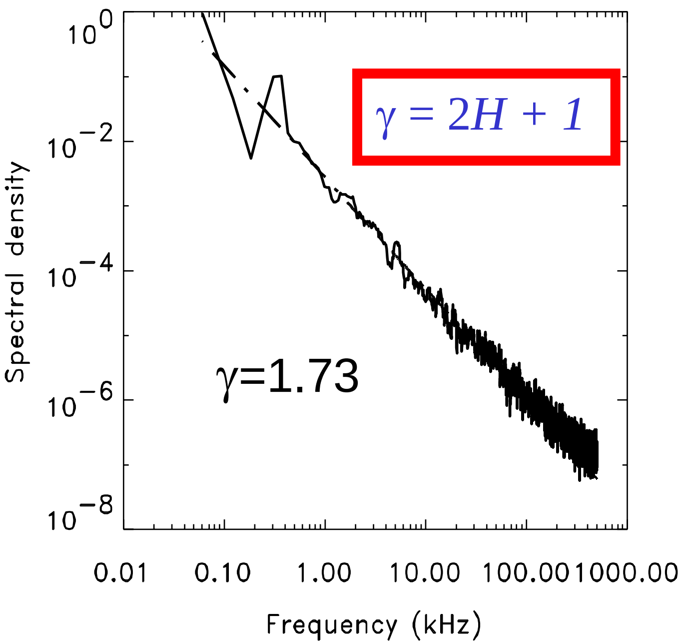

Example: the X_i are the increments (time derivative) of a fractional Brownian motion (fBm)

with H = 0.35

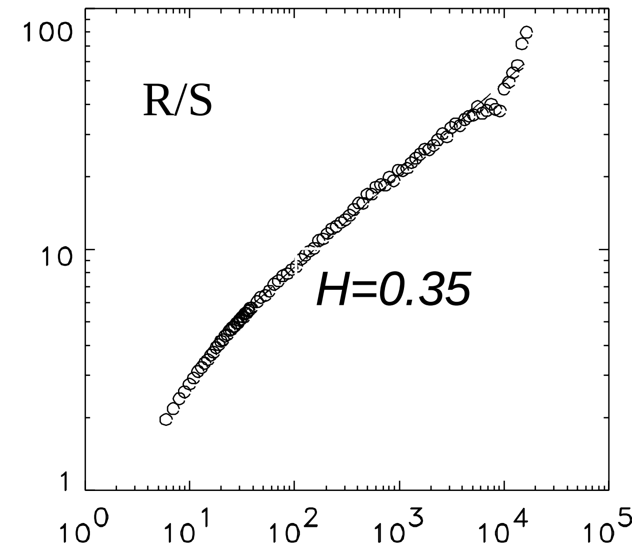

Drawback of the method: H must be in the range [0-1] $\Rightarrow \gamma = 2H + 1$ in the range: [1, 3] (R/S analysis on increments) or [-1,+1] (R/S analysis on signal)

Fractals and Wavelets

Wavelets are self-similar by nature

Mother-wavelet $\varphi(t)$ $\Rightarrow$ $\varphi_{T,t_0}(t) = \varphi\left(\frac{t-t_0}{T}\right)$ translation + dilatation

- The **wavelet variance** is a very useful alternative to spectral density function, and R/S analysis

- Discrete wavelet transform

  octave scaling $\rightarrow$ $T_m = 2^{m-1}$ $\Rightarrow$ $\nu_X^2(\tau_j) \equiv \mathrm{var}\left\{\overline{W_j}\right\}$ with $\tau_j = 2^{j-1}$

$$\sum_{j=1} \nu_X^2(\tau_j) \equiv \sigma_X^2$$

$$\nu_X^2(\tau_j) \approx \int_{1/2^{j+1}}^{1/2^j} S_X(f)\,df$$

$$\Rightarrow \text{(if } S_X(f) \propto |f|^{\alpha} \text{)} \quad \nu_X^2(\tau_j) \propto \tau_j^{-\alpha-1} \quad \Rightarrow$$

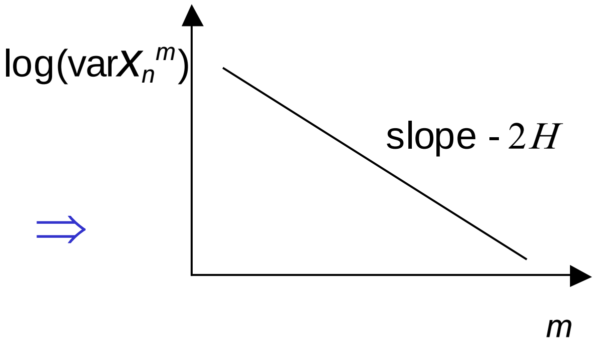

Wavelet variance (DWT, Daubechies D20)

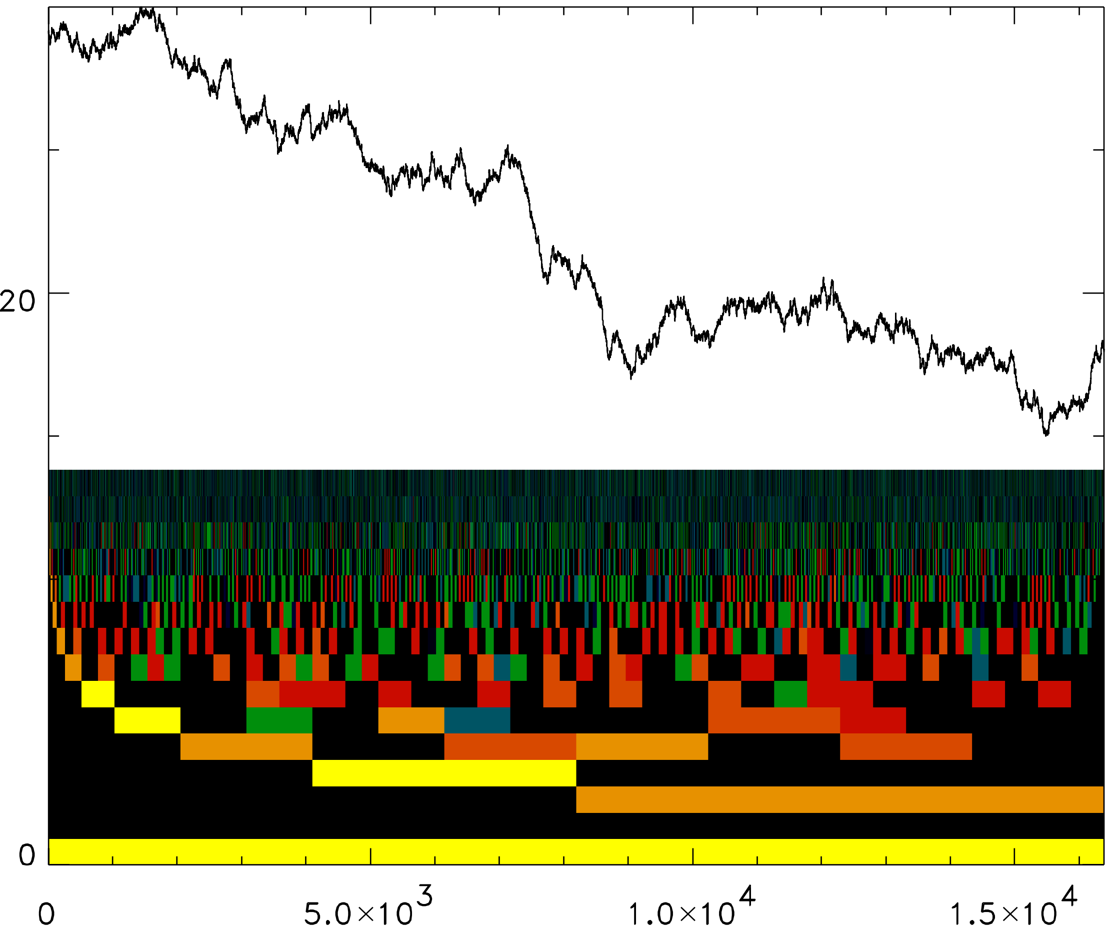

Brownian motion (H = 0.5)

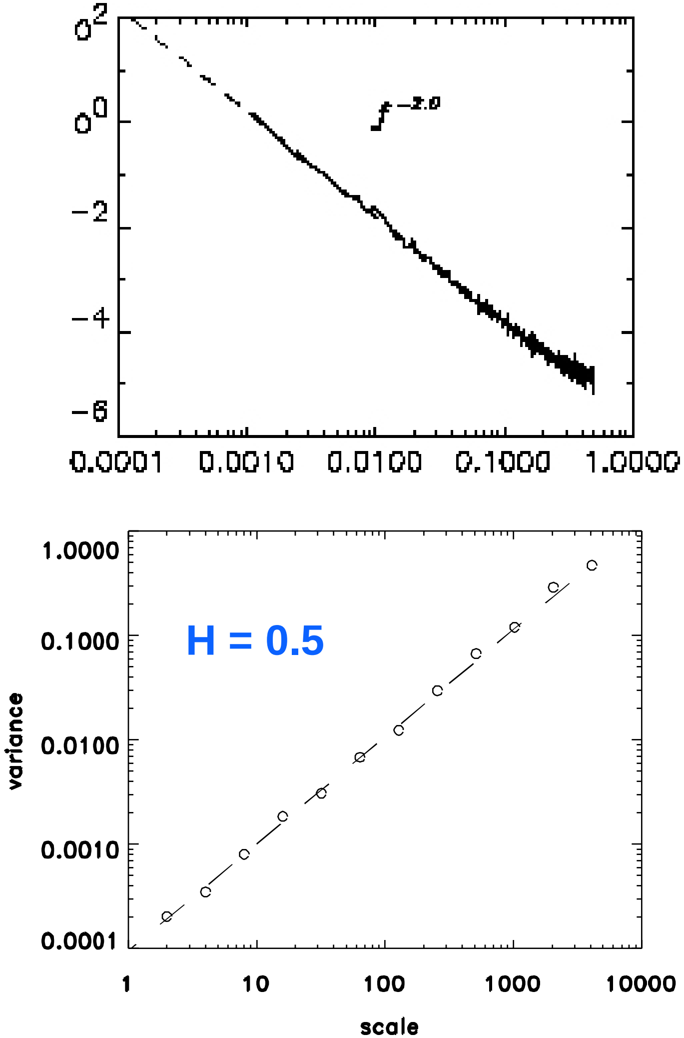

Variance of wavelet coefficients

SOL turbulence (Tore-Supra data)

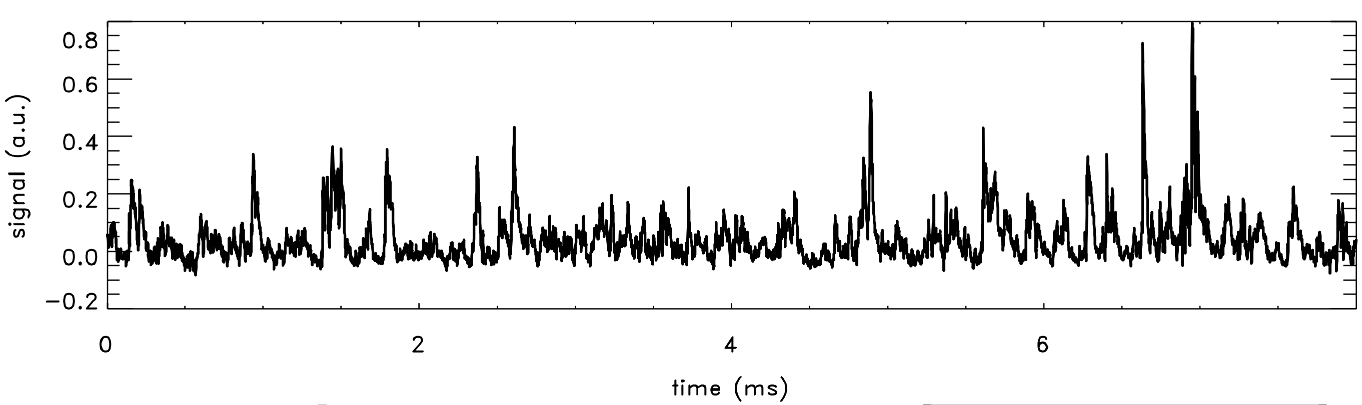

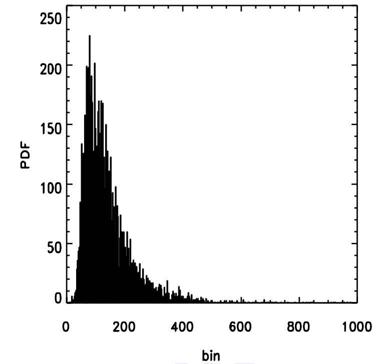

PDF

Tore-Supra: shot #22253

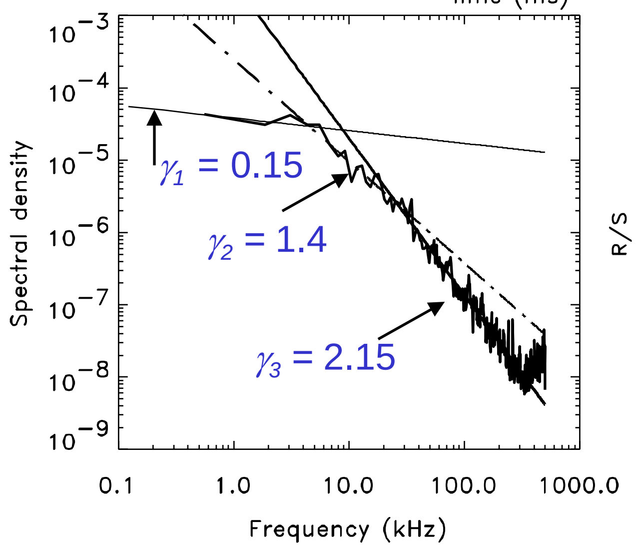

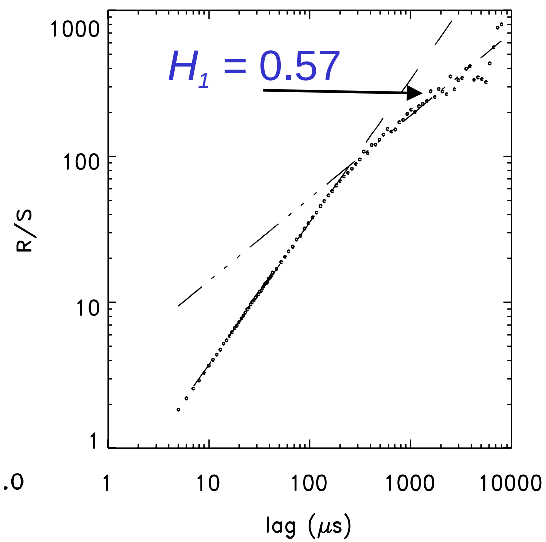

Signal: H_1 = 0.57

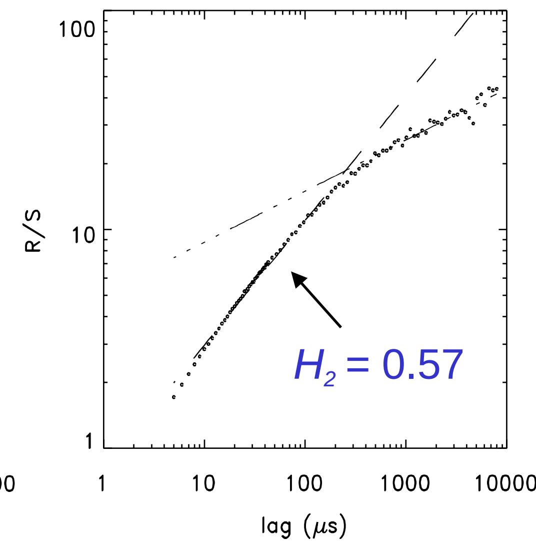

Increments H_2 = 0.57

Two distinct behaviors can be seen on the spectrum:

- before breakpoint (BF) signal ~ fGn
- After breakpoint (HF) signal ~ fBm

Question :
Why such a relationship ?

Tore-Supra (Shot #35000)

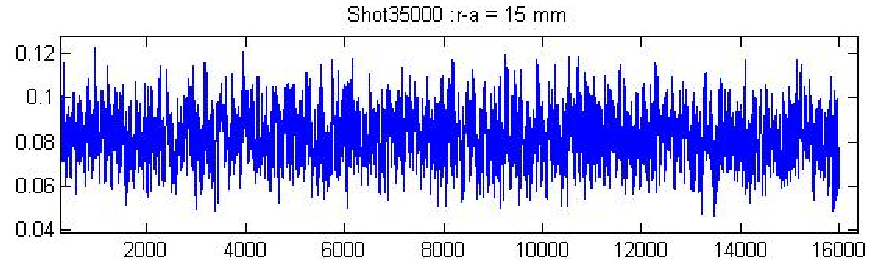

2B Isat,

x_m = 0,0822

σ = 0,0118

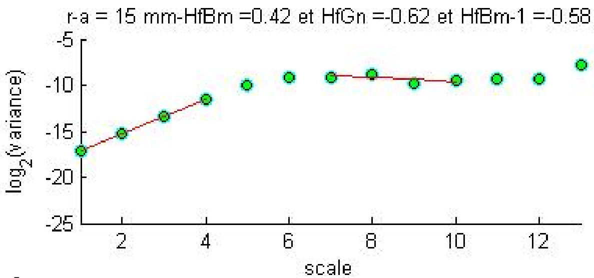

γ=1.84

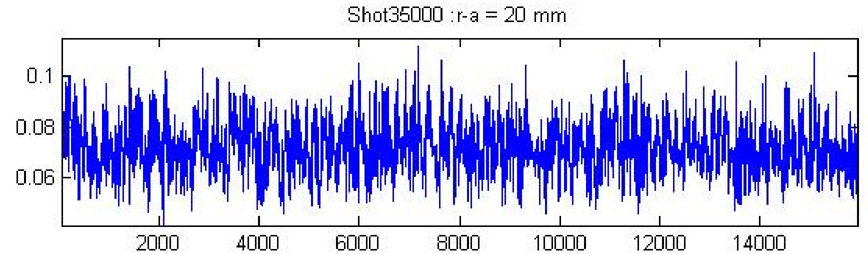

2B Isat,

x_m = 0,072

σ = 0,0094

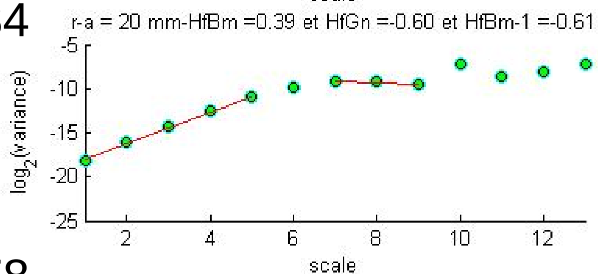

γ=1.78

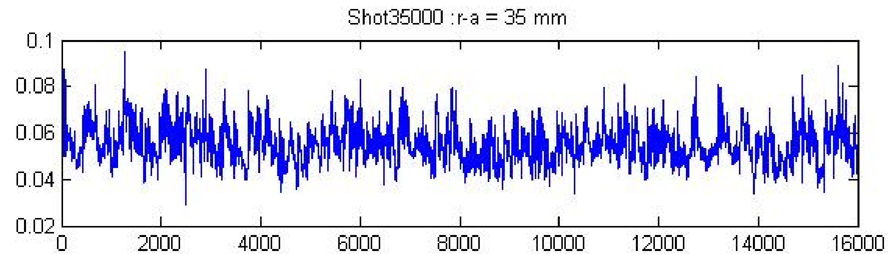

2B Isat,

x_m = 0,0551

σ = 0,0076

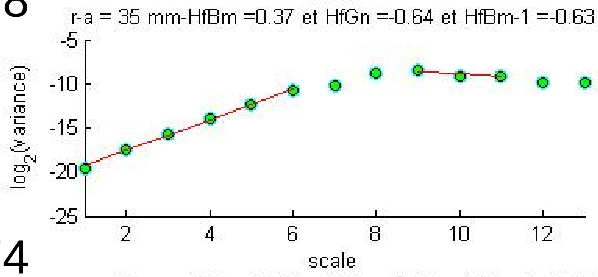

γ=1.74

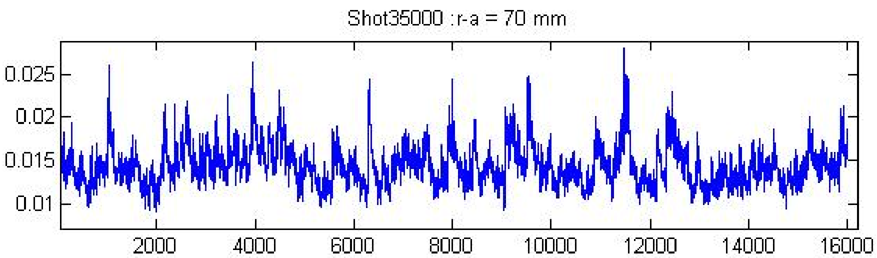

2B Isat,

x_m = 0,0144

σ = 0,0023

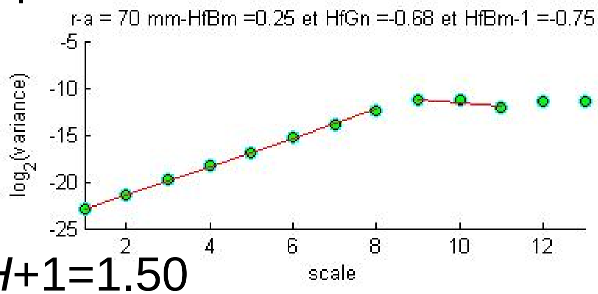

$\gamma = 2H + 1 = 1.50$

Continuous wavelets: Time-frequency analysis

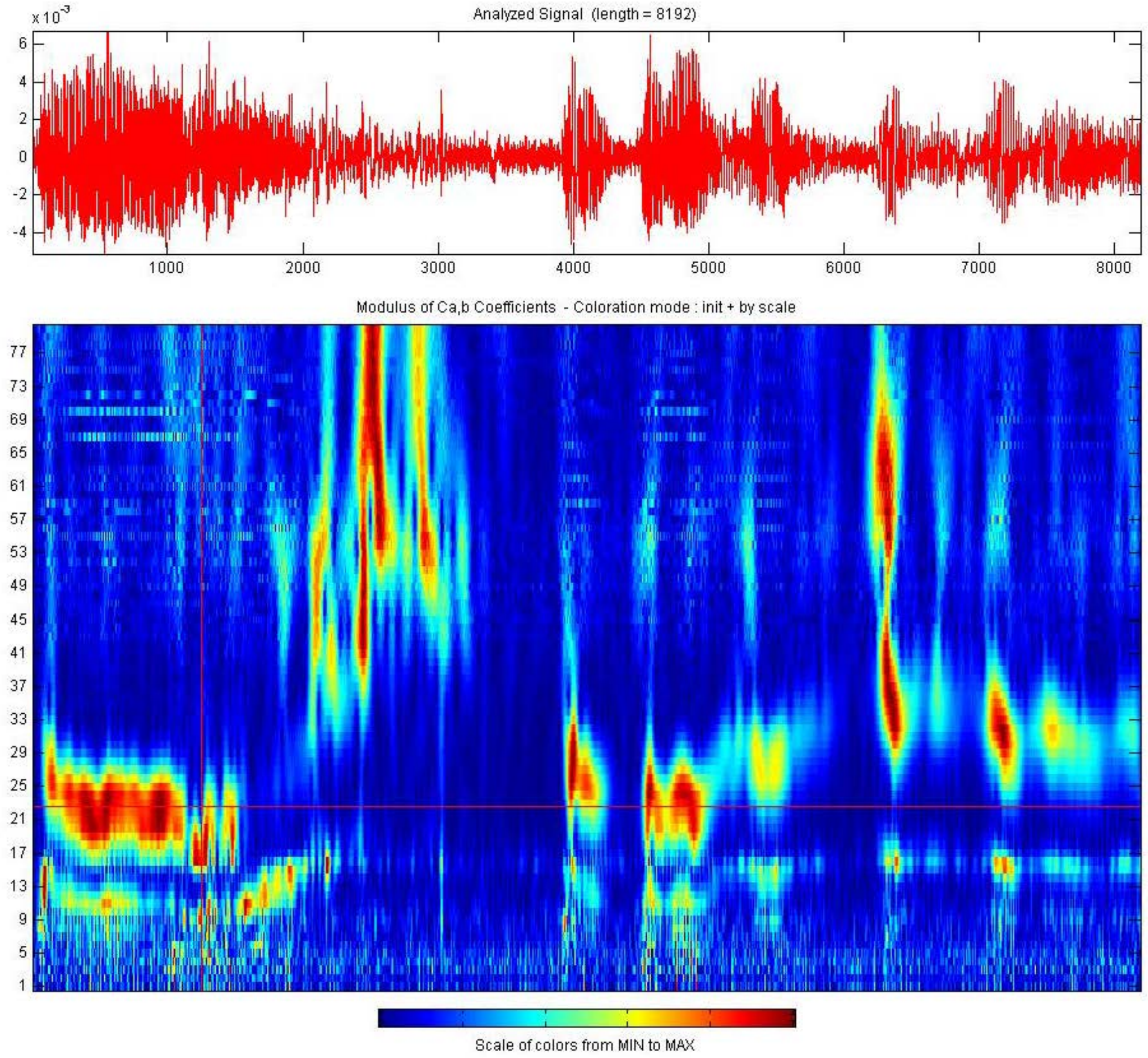

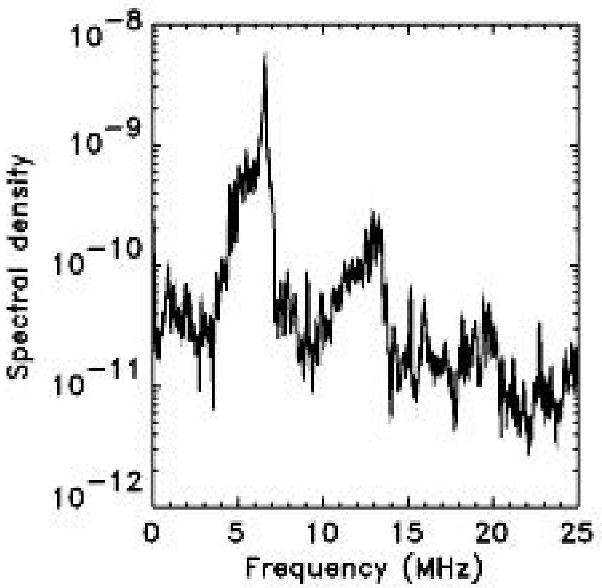

Fourier spectrum

Pivoine data
(from A. Lazurenko)

Time-frequency representation obtained with Morlet wavelets

Drawback → cpu time demanding (because high level of redundancy)

Discrete wavelets: Analysis and reconstruction

Daubechies wavelets

Analysis

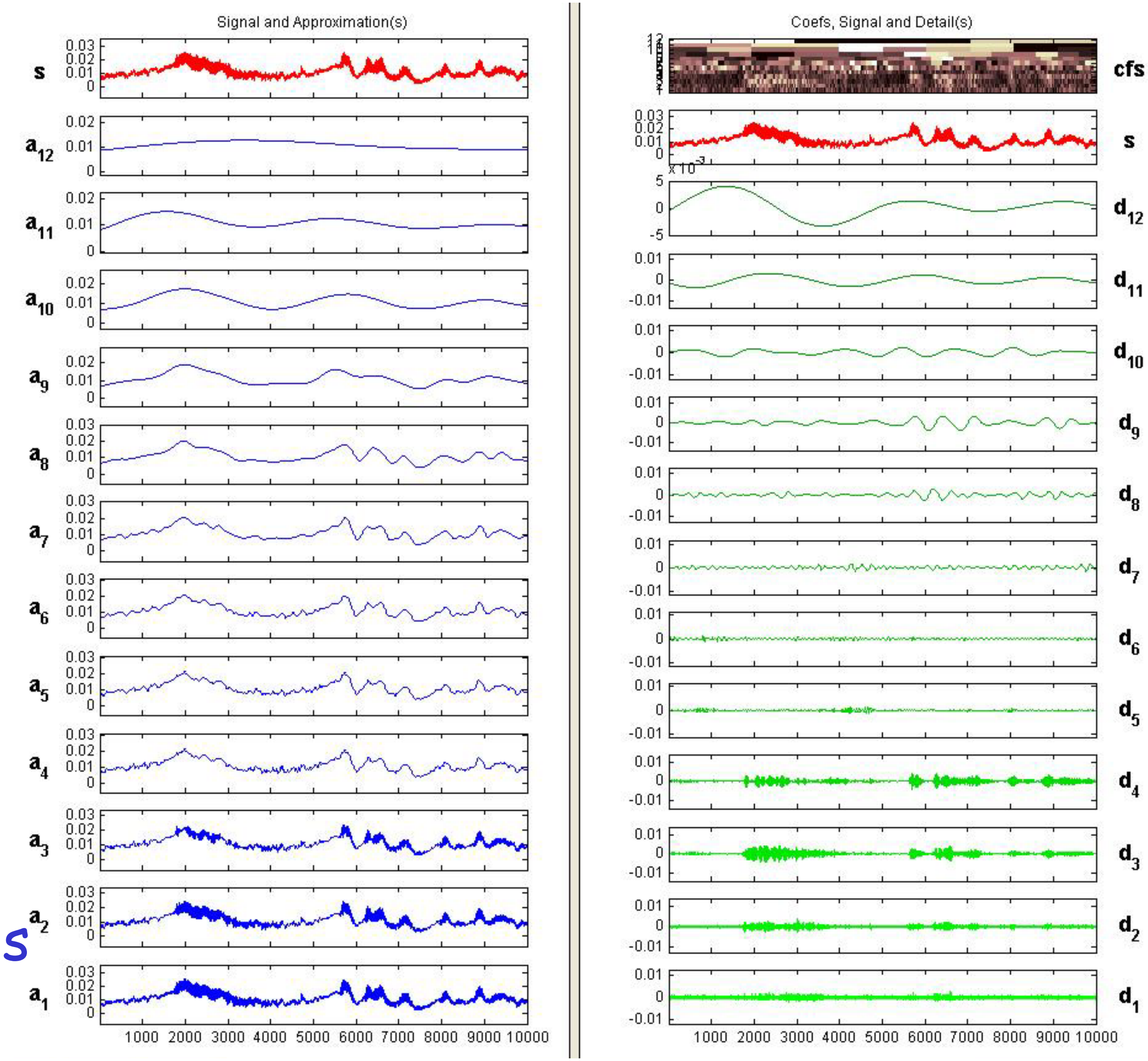

Synthesis

Efficient algorithmn,
But:
- physical meaning of the filtering?
- not well suited to time frequency analysis

The Hilbert-Huang Transform or Empirical Mode Decomposition

- Decomposition of a non stationary time-series into a finite sum of orthogonal eigenmodes, or Intrinsic Mode Functions (IMF).
- Self adaptive approach in which the eigenmodes are derived from the specific temporal behaviour of the signal.
- Subsequently, the Hilbert Transform can be used to compute the instantaneous frequency and a time-frequency representation of each mode as well as a global marginal Hilbert energy spectrum.

N. E. Huang et al., *The Empirical Mode Decomposition and Hilbert Spectrum for Nonlinear and Non-Stationary Time Series Analysis*, Proc. R. Soc. London, Ser. A, **454**, pp. 903-995 (1998).

T. Schlurmann, *Spectral Analysis of Nonlinear Water Waves based on the Hilbert-Huang transformation,* Transactions of the ASME Vol.**124** (2002) 22.

J. Terradas et al, The Astrophys. Journal **614** (2004) 435.

P. Flandrin, G. Rilling, P. Gonçalves, *Empirical Mode Decomposition as a Filter Bank*, IEEE Sig. Proc. Lett., Vol.**11**, N°2, pp. 112-114 (2004).

Hilbert Transform and instantaneous frequency

Hilbert transform of a data series x(t) is defined by:

$$H[x(t)] = \frac{1}{\pi}\, p.v. \int_{-\infty}^{+\infty} \frac{x(u)}{(t-u)}\, du$$

By substituting $y(t) = H[(x(t)]$ we can define z(t) as the analytical signal of x(t)

$$z(t) = x(t) + iy(t) = A(t)\exp(i\theta(t))$$

$$\text{with} \quad A(t) = \sqrt{x(t)^2 + y(t)^2} \quad \text{and} \quad \theta(t) = \arctan\left(\frac{y(t)}{x(t)}\right)$$

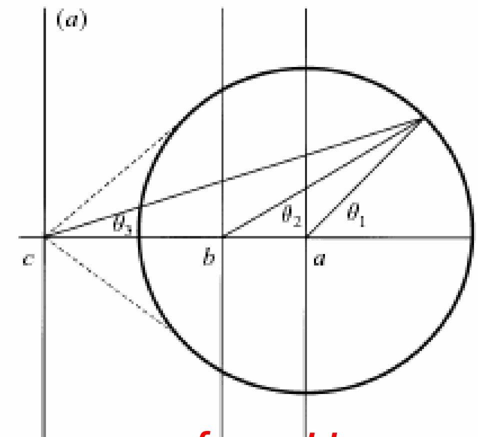

But in most cases the instantaneous frequency

$$\omega(t) = \frac{d\theta(t)}{dt}$$

has no physical meaning

from Huang et al

Example

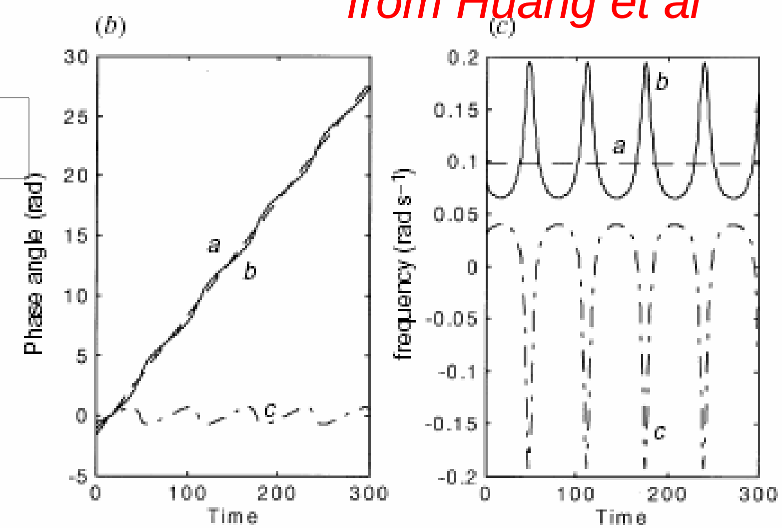

⇒ Empirical Mode Decomposition

set of IMF : (1) equal number of extrema and zero crossings; (2) mean value of the minima and maxima envelopes = 0

IMF = Intrinsic Mode Functions

The Empirical Mode Decomposition (sifting process)

1. **Initialize : $r_0(t) = X(t)$, j=1**
2. **Extract the j-th IMF:**
   - **a) Initialize $h_0(t) = r_j(t)$, k=1**
   - **b) Locate local maxima and minima of $h_{k-1}(t)$**
   - **c) Cubic spline interpolation to define upper and lower envelope of $h_{k-1}(t)$**
   - **d) Calculate mean $m_{k-1}(t)$ from upper and lower envelope of $h_{k-1}(t)$**
   - **e) Define $h_k(t) = h_{k-1}(t) - m_{k-1}(t)$**
   - **f) If stopping criteria are satisfied then $imf_j(t) = h_k(t)$ else go to 2(b) with k=k+1**
3. **Define $r_j(t) = r_{j-1}(t) - imf_j(t)$**
4. **If $r_j(t)$ still has at least two extrema then go to 2(a) with j=j+1, else the EMD is finished**
5. **$r_j(t)$ is the residue of x(t)**

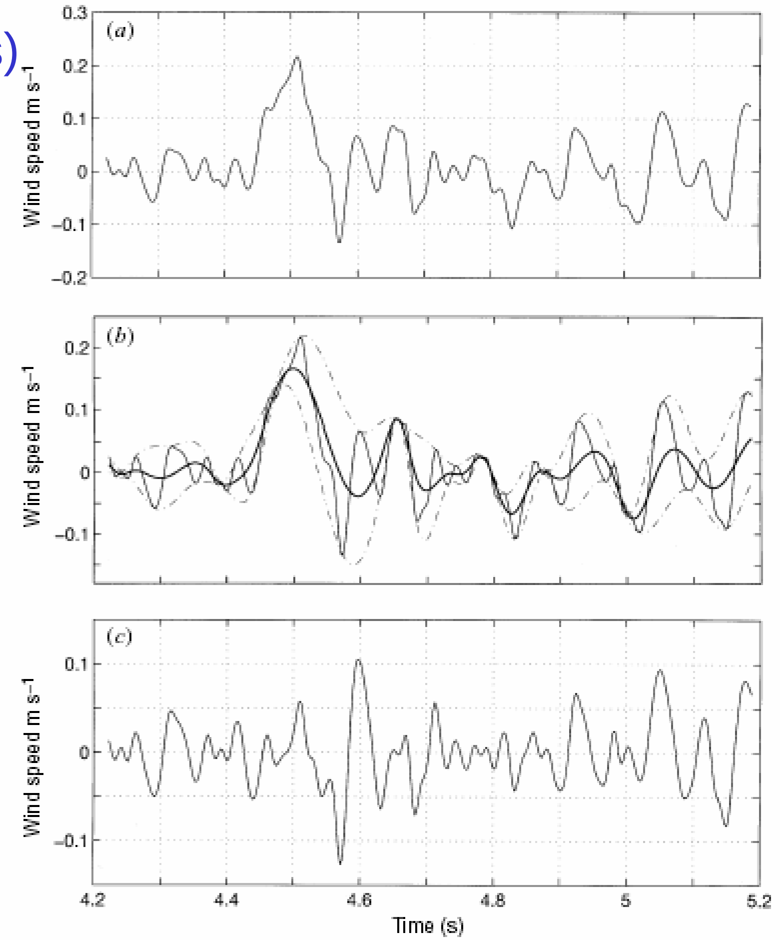

from Huang et al

$$\Rightarrow \quad X(t) = \sum_{j=1}^{n} imf_j(t) + r_n(t)$$

A typical IMF

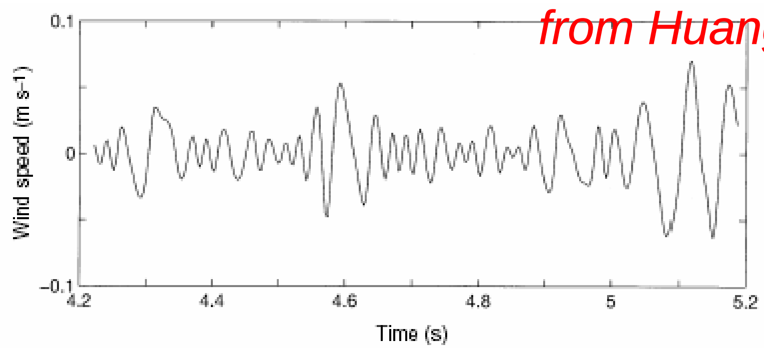

Analysis and Reconstruction (Plasma thruster data)

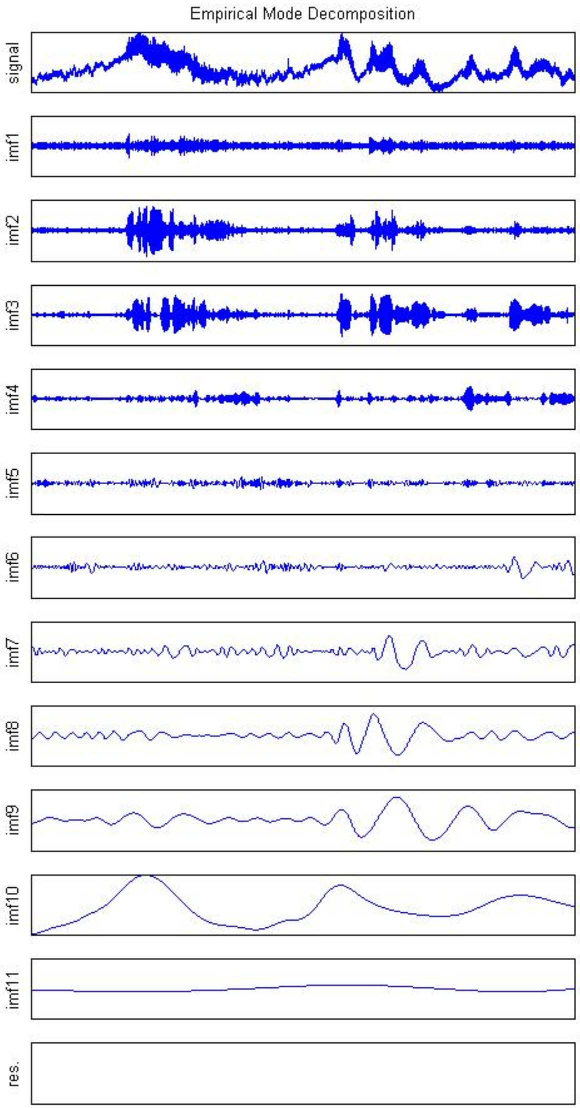

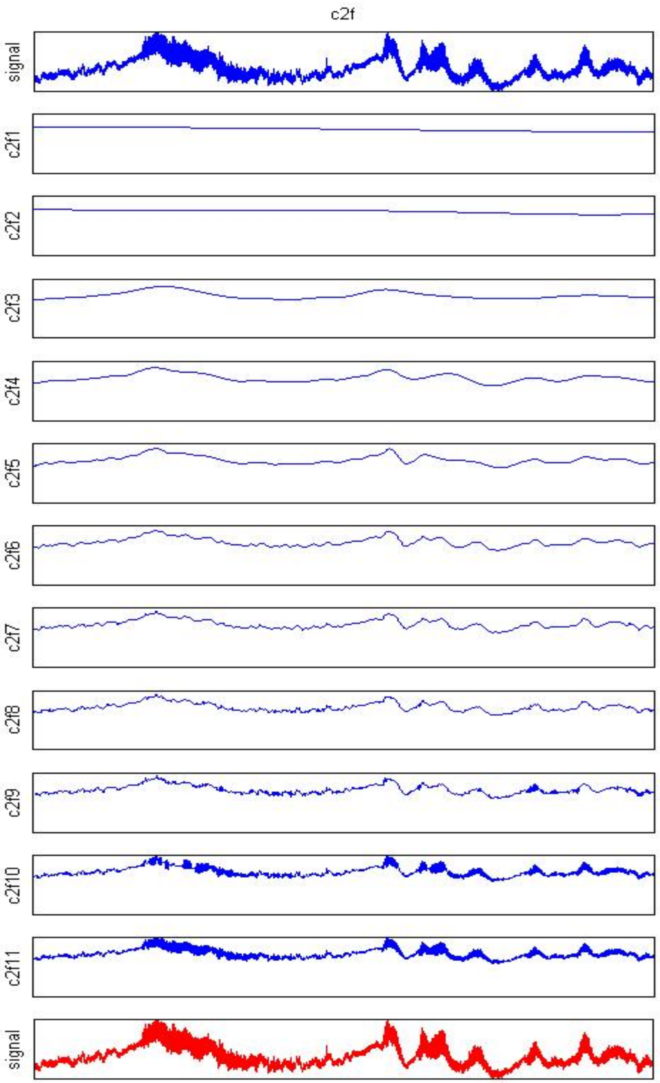

Analysis

Synthesis

Completeness and Orthogonality

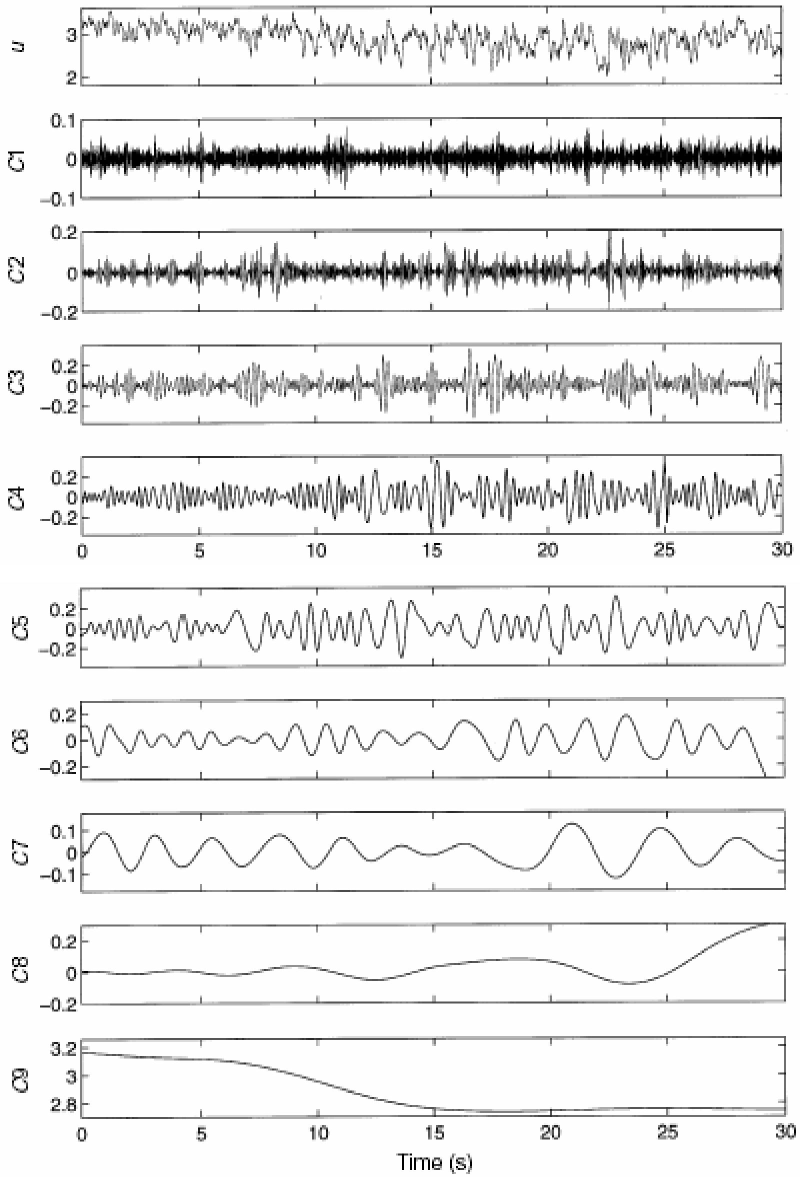

Example (from Huang et al)

The completeness is established both theoretically and numerically

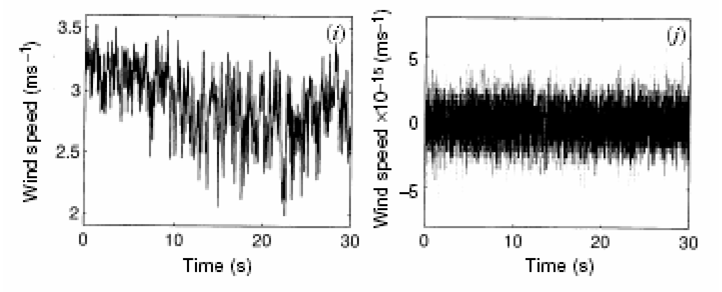

The orthogonality is satisfied in practical sense, but it is not guaranteed theoretically

$$X^2(t) = \sum_{j=1}^{n+1} C_j^2(t) + 2\sum_{j=1}^{n+1}\sum_{k=1}^{n+1} C_j(t)C_k(t)$$

IO = overall index of orthogonality

$$\mathrm{IO} = \sum_{t=0}^{T}\left(\sum_{j=1}^{n+1}\sum_{k=1}^{n+1} C_j(t)C_k(t)/X^2(t)\right)$$

for this example IO = 0.0067

or for two IMF: $\mathrm{IO}_{fg} = \sum_t \frac{C_f C_g}{C_f^2 + C_g^2}$

Degree of stationarity

The degree of stationarity DS is defined as:

$$DS(\omega) = \frac{1}{T}\int_0^T \left(1 - \frac{H(\omega,t)}{n(\omega)}\right)^2 \mathrm{d}t$$

with $n(\omega) = \frac{1}{T}h(\omega)$. mean marginal spectrum

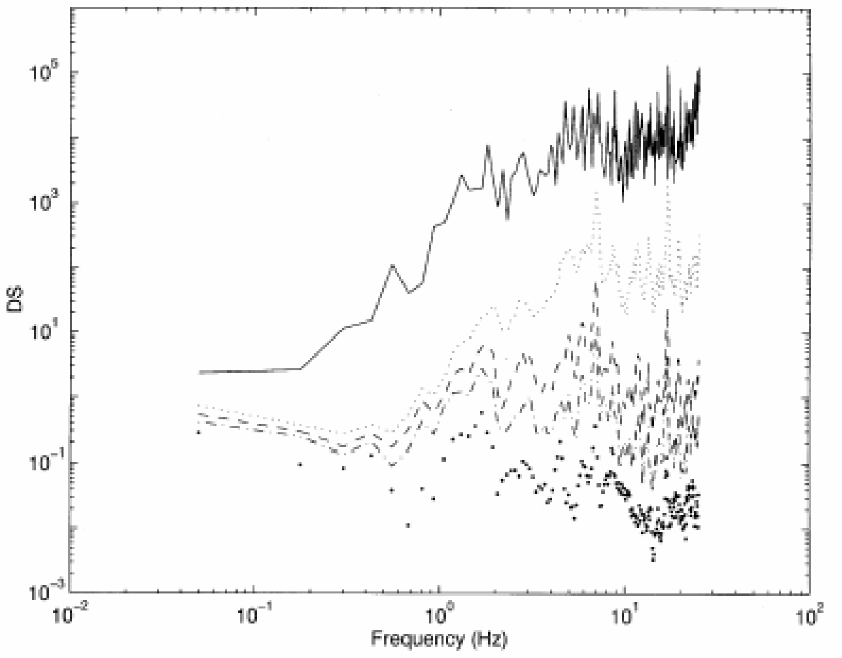

and the degree of statistic stationarity DSS can be is defined as:

$$DSS(\omega, \Delta T) = \frac{1}{T}\int_0^T \left(1 - \frac{\overline{H(\omega,t)}}{n(\omega)}\right)^2 \mathrm{d}t$$

If the Hilbert spectrum depends on time, the index will not be zero, then the Fourier spectrum will cease to make physical sense.
The higher the index value, the more non-stationary is the process.

Marginal Hilbert spectrum vs Fourier spectrum

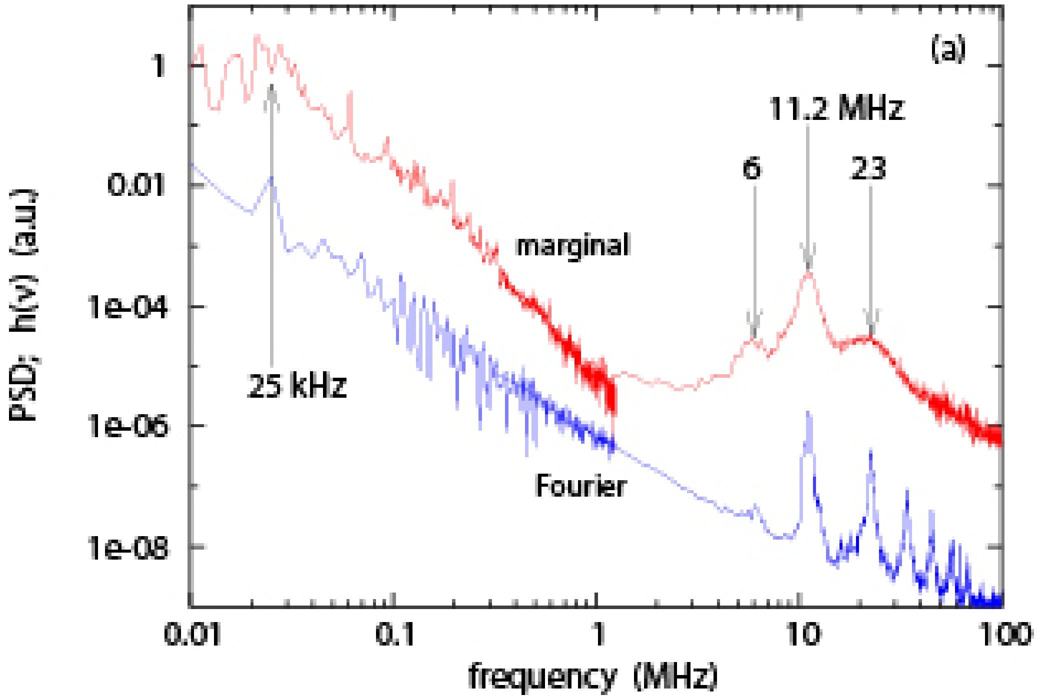

Because of the strong nonlinearity of HF oscillations the Fourier spectrum exhibits many peaks

All these peaks do not correspond to actual modes

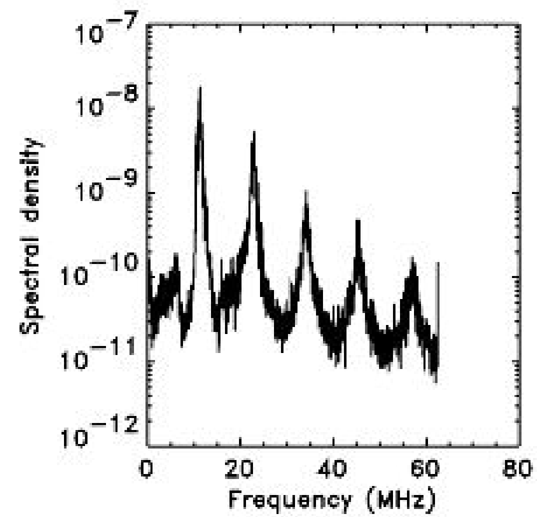

A peak in the marginal Hilbert spectrum corresponds to a whole oscillation around zero

Application to experimental time-series (Plasma Thruster)

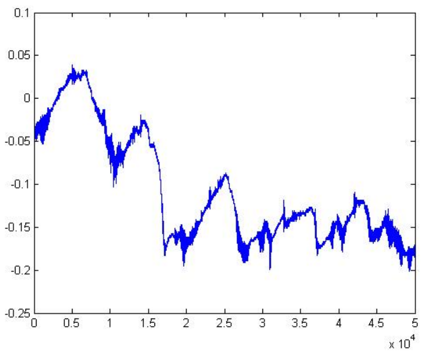

Analyzed Signal

J. Kurzyna et al.,
submitted to Phys. of Plasmas

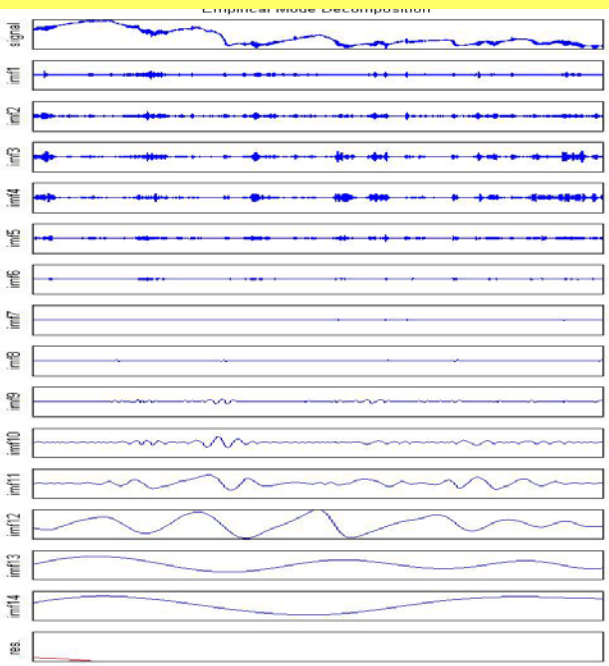

IMF 1-4

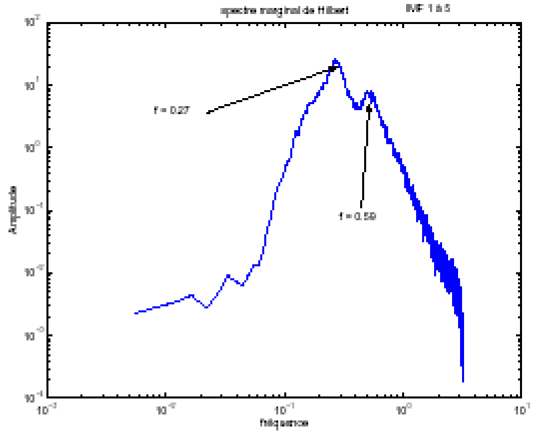

Marginal Hilbert Spectrum

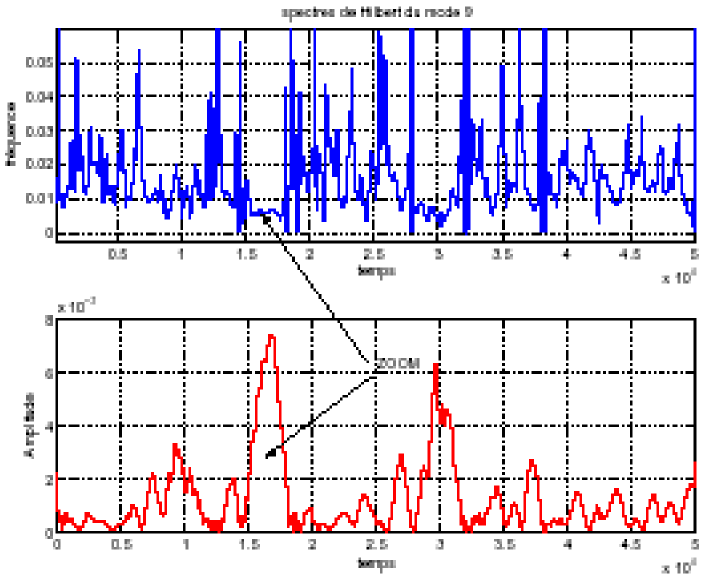

IMF 9

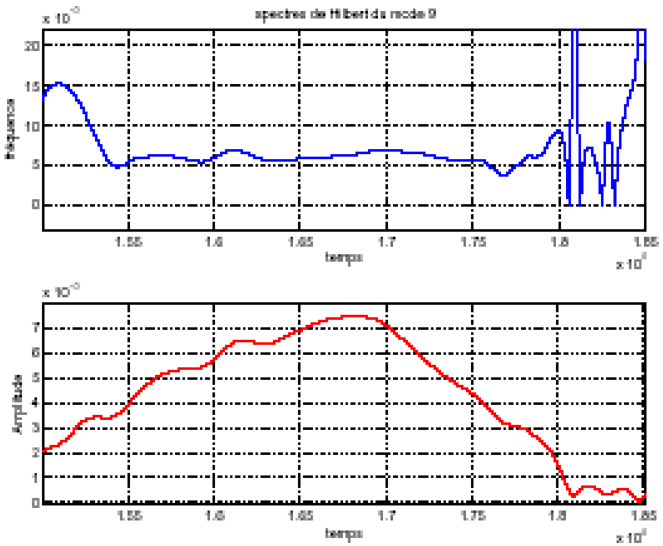

Comparison with wavelet time-frequency analysis

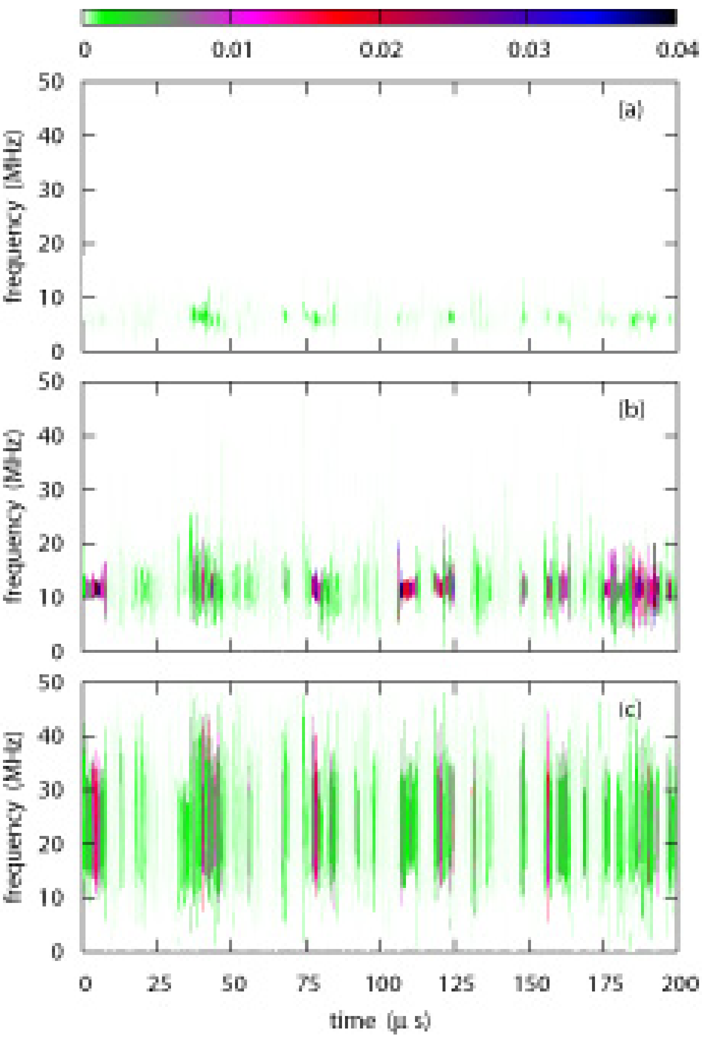

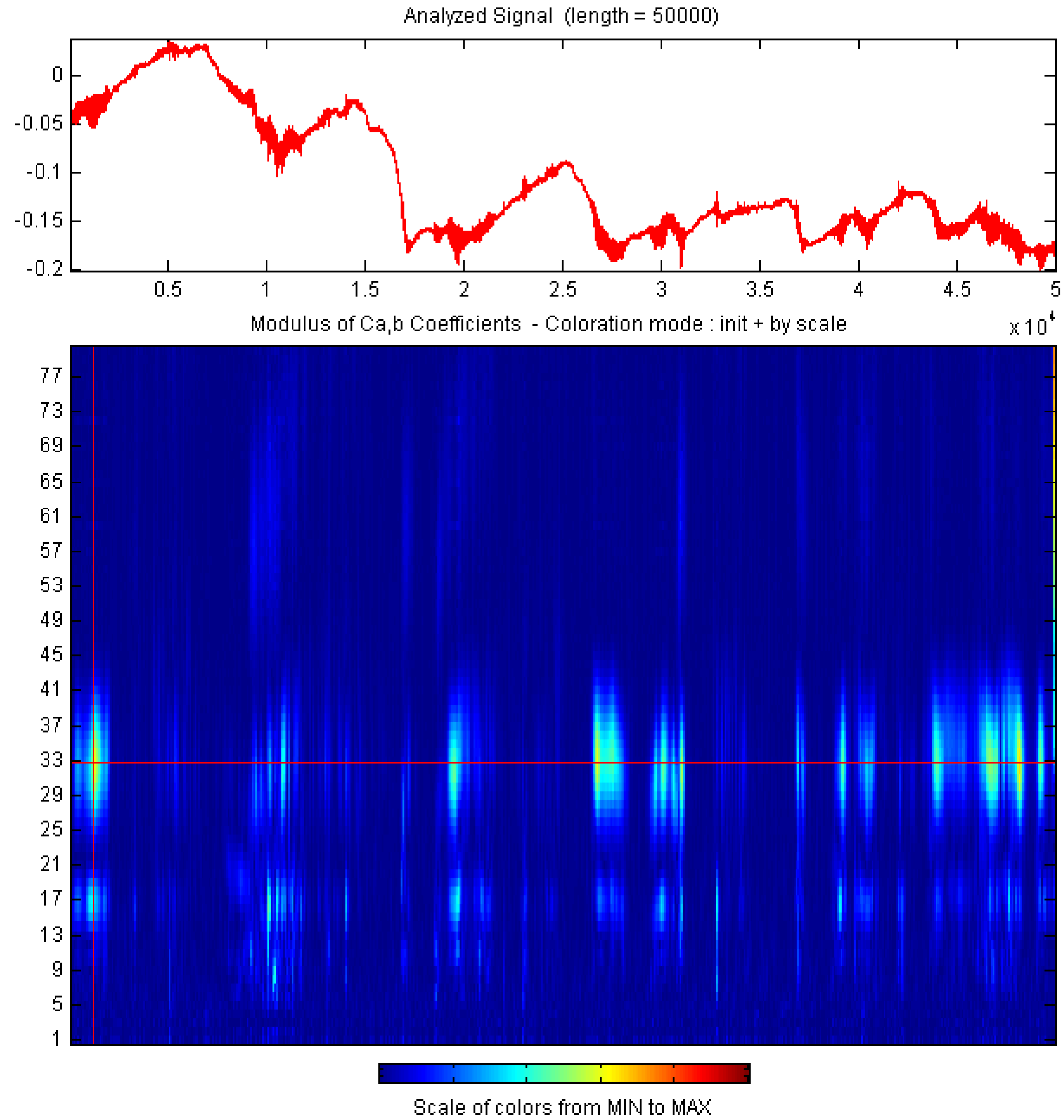

Morlet → freq. = 375/scale ⇒ 33 ↔ 11.4 MHz

Conclusions and Perspectives

The Hilbert-Huang Transform method:

- Has proven to be a promising and attractive method to analyze non stationary and nonlinear time-series because of:

  - a very efficient ability in filtering different physical phenomena

  - accurate time-frequency representation

  - moderate cpu time consumption and ability to analyse long time series

- Some improvements would be useful, e.g., Hilbert spectra representation

Linear spectral analysis tools

The classical Fourier analysis tools are redefined in terms of wavelets:

in order to obtain statistical stability, the appropriate combinations of wavelet coefficients are integrated over a small finite time interval

$f(t)$ is digitally sampled on $[0, N T_s]$

$$T_0 - \frac{T}{2} \le \tau \le T_0 + \frac{T}{2}$$

• Wavelet spectra and coherence

$$C_{fg}^W(a, T_0) = \int_T W_f^*(a,\tau) W_g(a,\tau) d\tau$$

• normalized delayed wavelet cross coherence

$$\gamma_{fg}^W(a, T_0, \Delta\tau) = \frac{\left| \int_T W_f^*(a,\tau) W_g(a,\tau+\Delta\tau) d\tau \right|}{\left(P_f^W(a, T_0) P_g^W(a, T_0 + \Delta\tau) \right)^{1/2}}$$

→ estimate of the statistical noise level

$$\varepsilon(\gamma_{fg}^W) \approx \left[\frac{\omega_s}{\omega} \frac{1}{N} \right]^{1/2}$$

where $P_f^W(a, T_0) = C_{ff}^W(a, T_0)$ is the wavelet auto-power spectrum

Joint wavelet phase-frequency spectra

- The Joint wavelet phase-frequency spectrum $S(\phi, \omega)$ is obtained by calculating the quantity:

$$c = W_f^*(a,\tau) W_g(a, \tau + \Delta\tau)$$

for a number of values of a and τ, with fixed $\Delta\tau$

$\omega = 2\pi/a$ and ϕ phase of c $\rightarrow$ plot in the (ϕ, ω)-plane

$\Rightarrow$ insight into the frequency-dependent phase relations that may exist between f and g (usually two spatially separated measurements of the same quantity)

moreover (if homogeneous turbulence)

$\rightarrow$ related to the dispersion relation $\omega(k)$ for the process driving the turbulence

Non linear spectral analysis tools

Non linearity requires proper spectral analysis tools :

The Fourier method is based on the third-order spectrum $B_{fg}(\omega_1,\omega_2)=\left\langle F^*(\omega)G(\omega_1)G(\omega_2)\right\rangle$

where $\omega = \omega_1 + \omega_2$ and <·> = ensemble average

- Wavelet cross bispectrum $$B^W_{fg}(a_1,a_2,T_0)=\int_T W^*_f(a,\tau)W_g(a_1,\tau)W_g(a_2,\tau)d\tau$$
- Wavelet cross bicoherence (normalized squared cross bispectrum)

$$\left(b^W_{fg}(a_1,a_2,T_0)\right)^2=\frac{\left|B^W_{fg}(a_1,a_2,T_0)\right|^2}{\left(\int_T\left|W_f(a_1,\tau)W_g(a_2,\tau)\right|^2 d\tau\right)P^W_f(a,T_0)}$$

- Wavelet auto bispectrum and auto bicoherence $B^W(a_1,a_2,T_0)=B^W_{ff}(a_1,a_2,T_0)$
  and $\left(b^W(a_1,a_2,T_0)\right)^2=\left(b^W_{ff}(a_1,a_2,T_0)\right)^2$

•The bicoherence is a measure of the amount of phase coupling that occurs in a signal or between two signals. Advantage of wavelet bicoherence $\rightarrow$ ability to detect temporal variations in phase coupling (intermittent behaviour)

Bicoherence as a Fourier tool

Test Signal Bicoherence

- We consider a test signal of the following form to demonstrate tl importance of coherent phases in bispectral analysis:

$$y(t) = \sin(\omega_1 t + \theta_1) + \sin(\omega_2 t + \theta_2) + \sin(\omega_3 t + \theta_3),$$
$$\omega_1 = 0.1,\ \omega_2 = 0.25,\ \omega_3 = \omega_1 + \omega_2 = 0.35$$

$\theta_3 = \theta_1 + \theta_2$

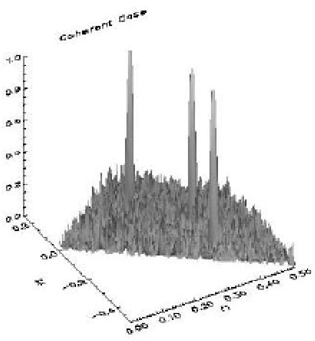

θ_3 random

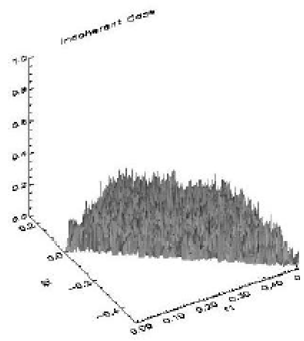

Test Signal Summed Bicoherence

- Calculate summed bicoherence as function of $\mathbf{f_3}$ along line $\mathbf{f_2 = f_3 - f_1}$. It corresponds to the total coherence between a frequency $\mathbf{f_3}$ and all other frequencies.
- See three spikes for the coherent case, corresponding to the three frequencies, and noise in the incoherent case.

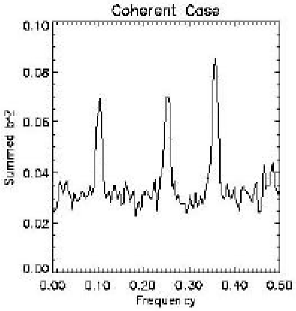

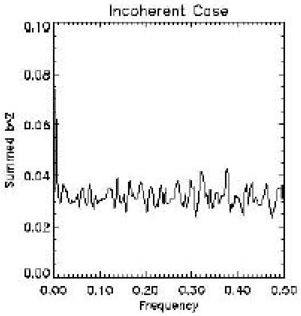

From Van Milligen, Wavelets in Physics, edited by J. C. Van Den Berg, (Cambridge University Press, 1999)

Example: coupled van der Pol oscillators (1)

$$\begin{cases} \dfrac{\partial x_i}{\partial t} = y_i \\ \dfrac{\partial y_i}{\partial t} = \left[\varepsilon_i - \left(x_i + \alpha_i x_j\right)^2\right] y_i - (x_i + \alpha_i x_j) \end{cases}$$

Periodic state:

$\varepsilon_1 = 1.0 \quad \alpha_1 = 0.49$

$\varepsilon_2 = 1.0 \quad \alpha_2 = -1.75$

Chaotic state:

$\varepsilon_1 = 1.0 \quad \alpha_1 = 0.5$

$\varepsilon_2 = 1.0 \quad \alpha_2 = 1.75$

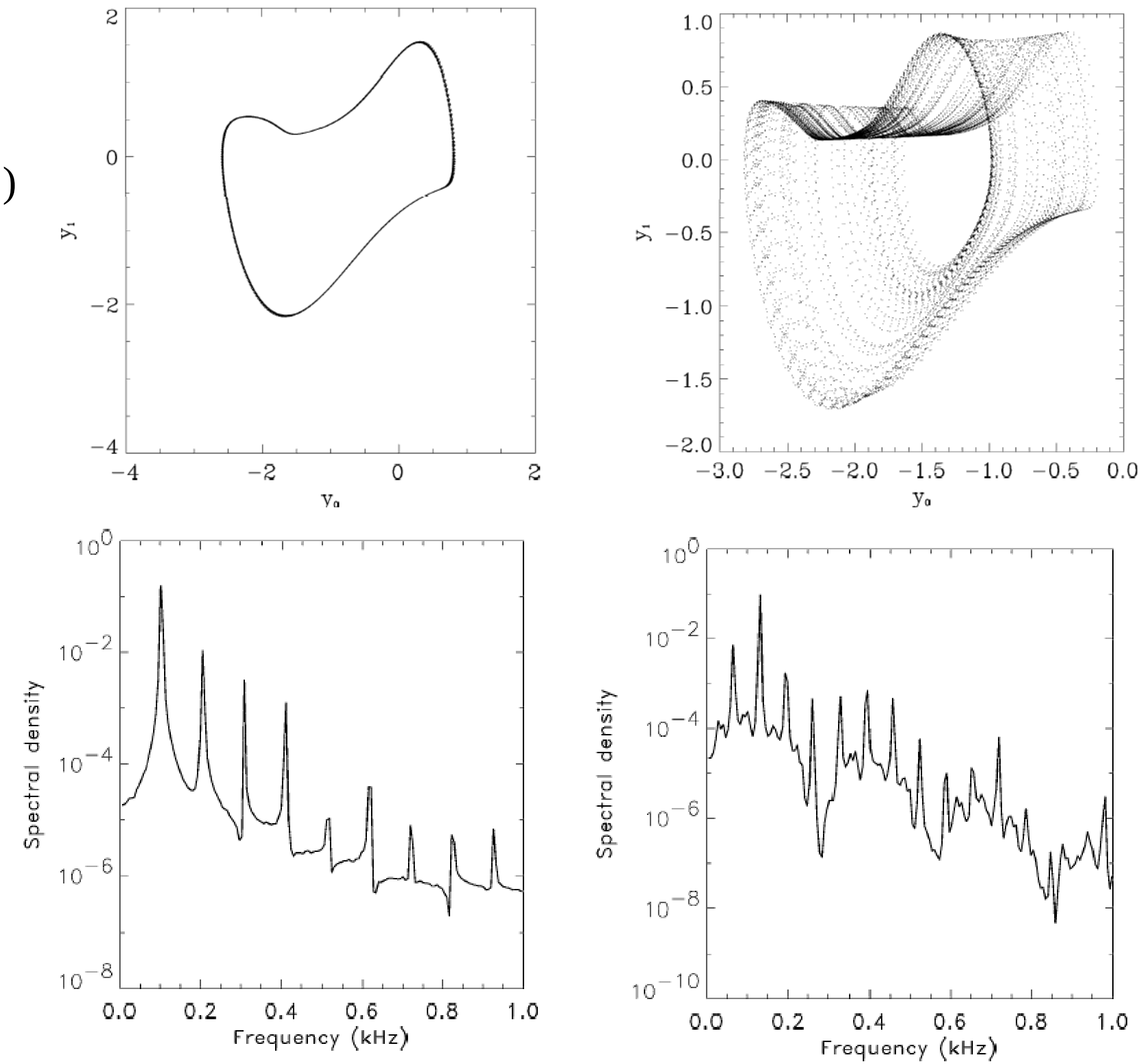

Example: coupled van der Pol oscillators (2)

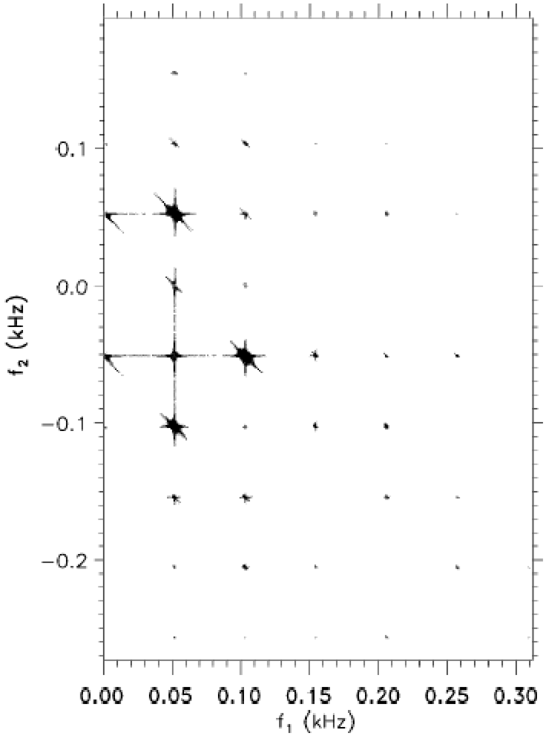

Periodic state:

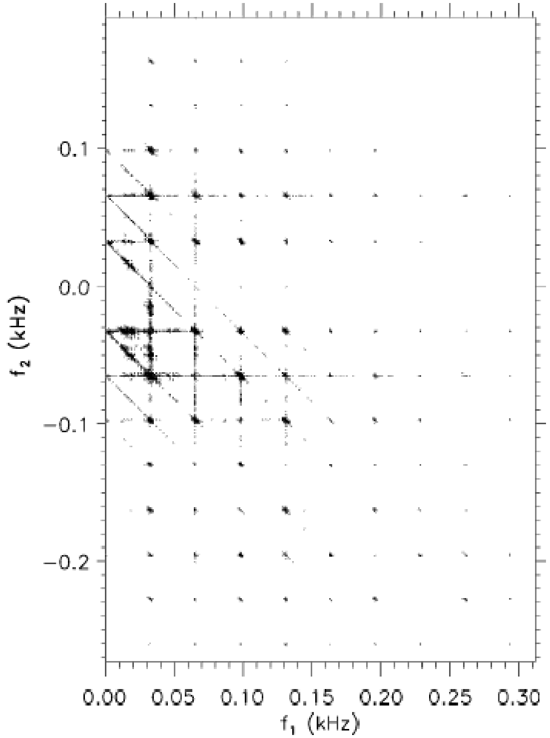

Chaotic state:

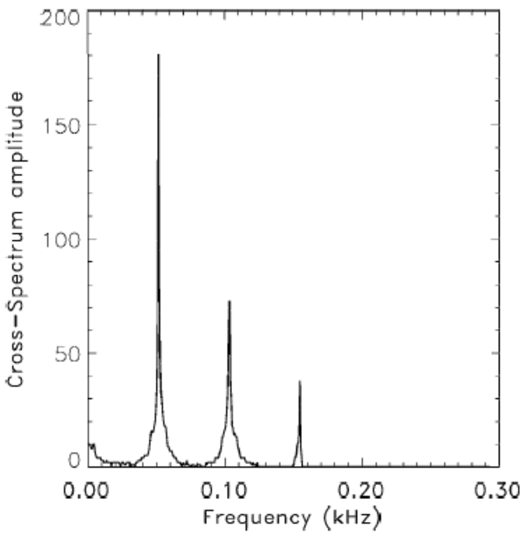

Summed bicoherence

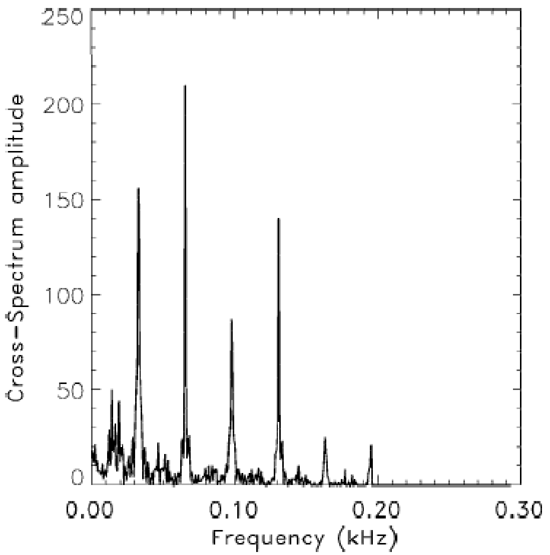

Fourier Bicoherence

Example: coupled van der Pol oscillators (3)

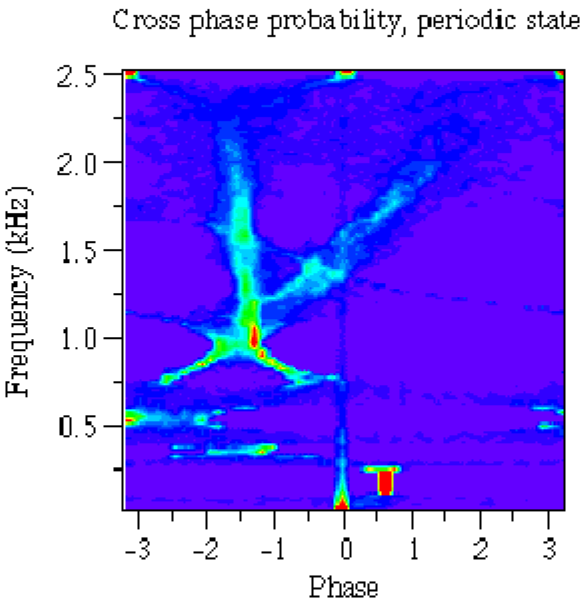

Periodic state: $\varepsilon_1 = 1.0$ $\varepsilon_2 = 1.0$ $\alpha_1 = 0.5$ $\alpha_2 = -1.75$

$\Leftarrow$ *Average phase relation between the two coordinates of one oscillator at every frequency $\Rightarrow$ low-dimensional attractor*

The bicoherence allows the determination of the driving frequency.

i.e., peak at $f = 0.34$ in the spectrum

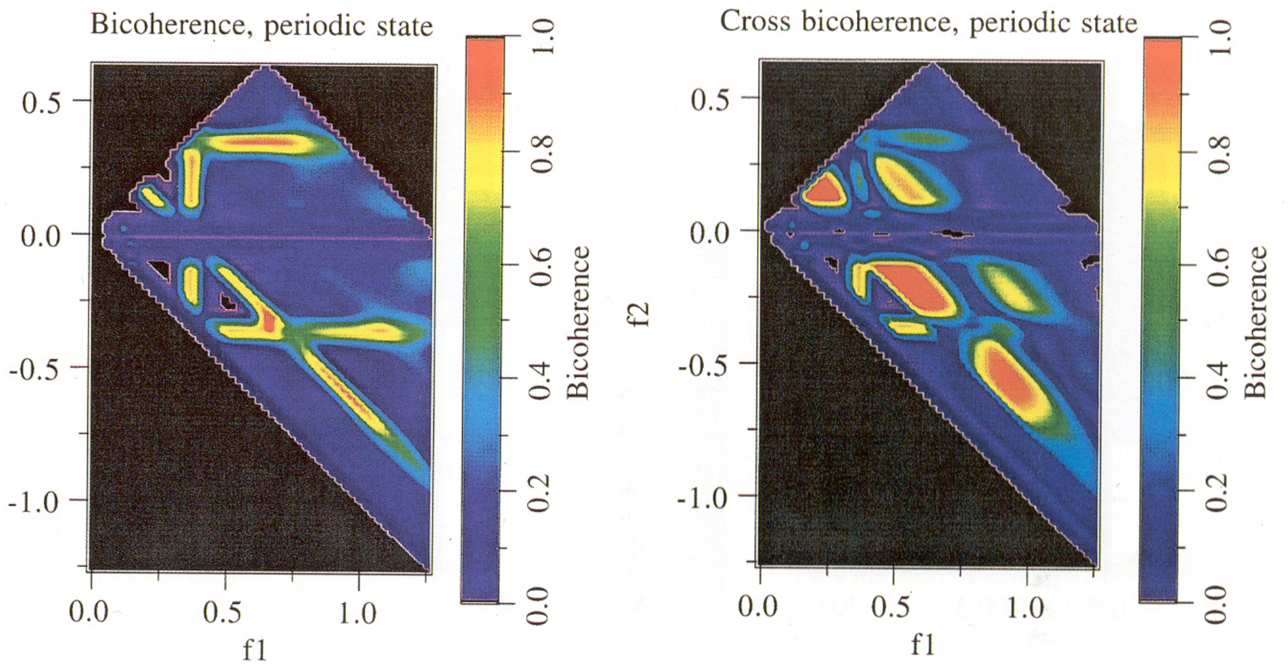

From van Milligen

Bicoherence analysis

Bispectrum of a spatial series S(x) :

$$B^W(a_1,a_2) = \int W_s^*(a,X)W_s(a_1,X)W_s(a_2,X)dX$$

$W_s(a,X)$= wavelet transform of S(x).

a, a_1, a_2 = wavelet scales such that $1/a = 1/a_1 + 1/a_2$

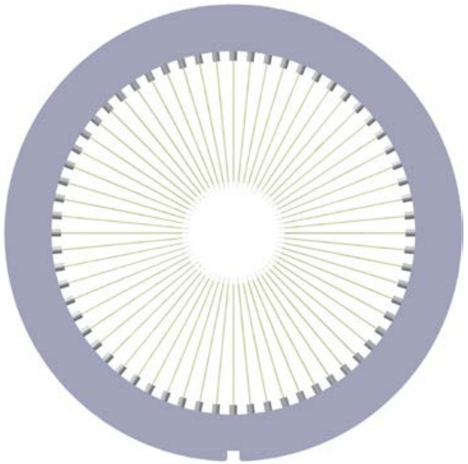

n=64, F_{ech} =1.25 MHz

B^W is a measure of the degree of nonlinear coupling between 3 waves satisfying the resonance condition :

$$\begin{cases} \omega_1 + \omega_2 = \omega_3 \\ k_1 + k_2 = k_3 \\ \Phi_1 + \Phi_2 = \Phi_3 + \text{const} \end{cases}$$

F. Brochard et al., Phys. Plasmas 13, 122305 (2006).

Bicoherence

Normalization of the bispectrum => Autobicoherence (bicoherence)

$$[b^W(a_1,a_2)]^2 = \frac{|B^W(a_1,a_2)|^2}{[\int |W_s(a_1,X)W_s(a_2,\tau)|^2 dX][\int |W_s(a,X)|^2 dX]}$$

$$0 \leq [b^W(a_1, a_2)]^2 \leq 1$$

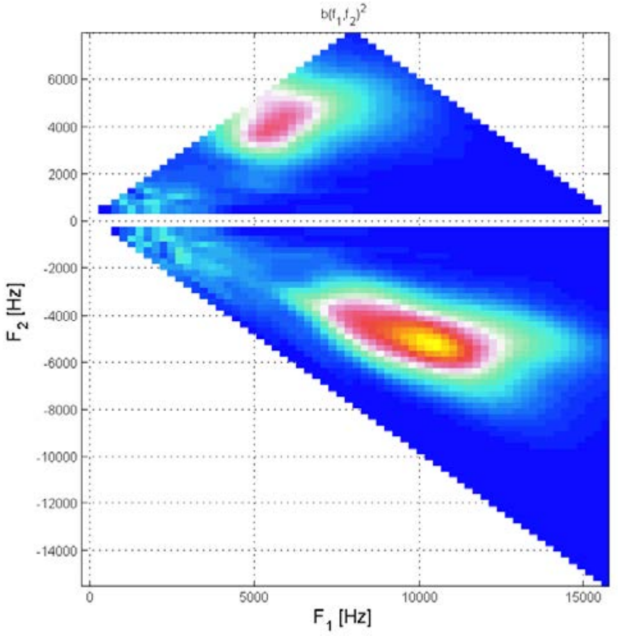

Auto-
Bicoherence

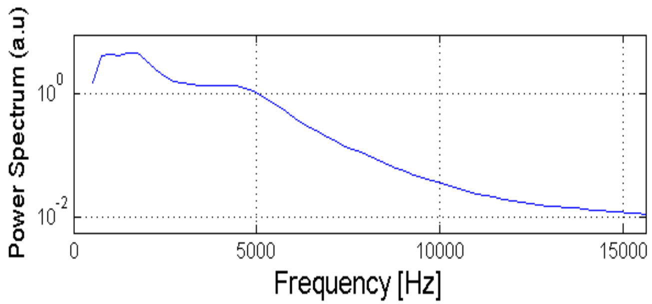

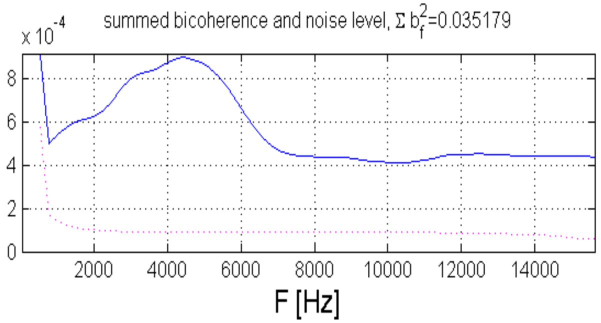

Summed
Bicoherence

Bicoherence

Summed Bicoherence

$$b^2(k_w) = \frac{1}{s} \sum_{k_u,k_v} b^2(k_u,k_v)\,\delta_{k_u+k_v,k_w}$$

allows to determine the coupling direction

Total bicoherence

$$b^2_{\mathrm{Tot}} = \frac{1}{S} \sum_{k_w} b^2(k_w)$$

gives an indication on the amount of nonlinear coupling

Staistical noise:

$$\epsilon[b^W(k_1,k_2)]^2 = \frac{1}{N \min(|k_1|,|k_2|,|k_1+k_2|)} \frac{1}{2\Delta x}$$

=> depends on the scale $1/k$

Results: dynamical analysis

Weakly turbulent state (drift waves) in the Vineta device

Density fluctuations

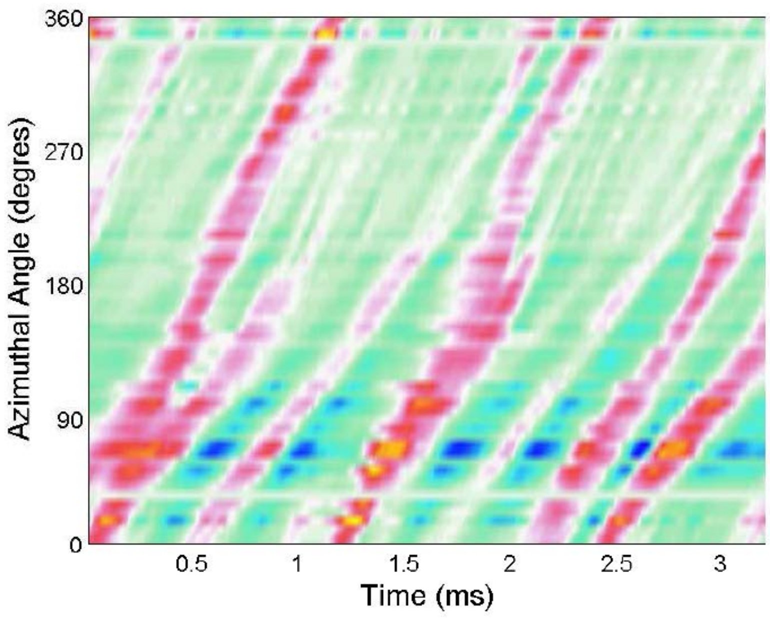

Time-series and PDF

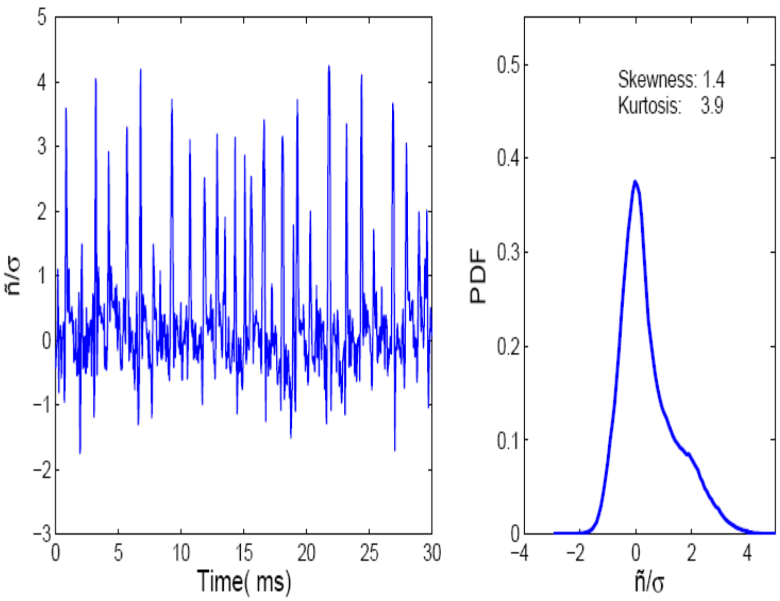

F. Brochard et al., Phys. Plasmas 13, 122305 (2006).

Results : dynamical analysis

More details are seen in the k spectrum than in the frequency spectrum (wavelet spectra).

Time/frequency spectrum

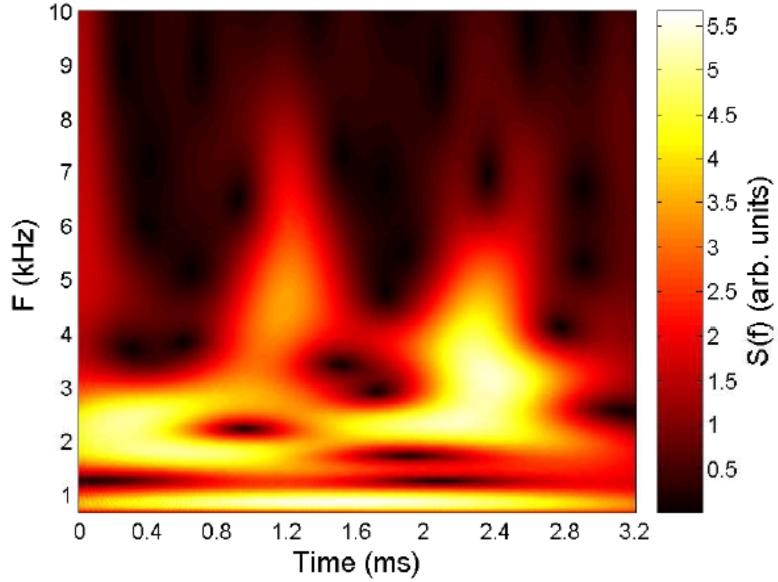

Time/wave number spectrum

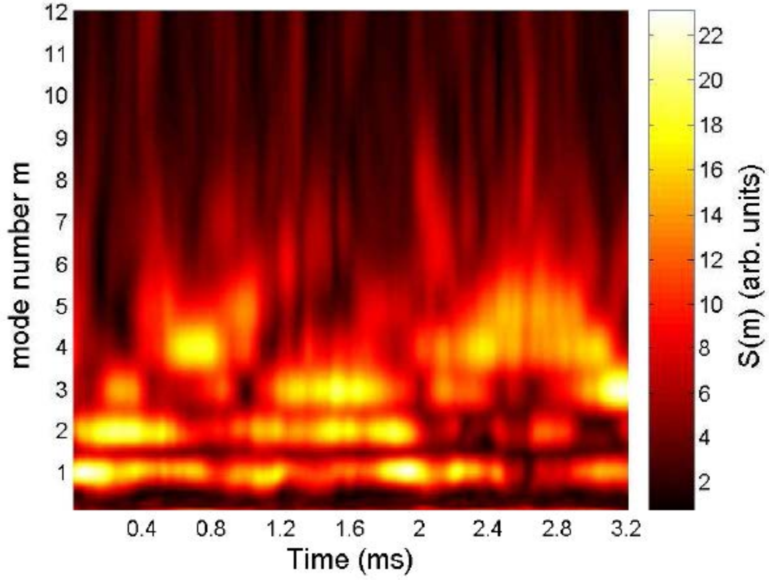

Results : dynamical analysis

The temporal evolution of the *k* total bicoherence shows bursts on small time scale (too small to be detected from a frequency analysis (~ T/10).

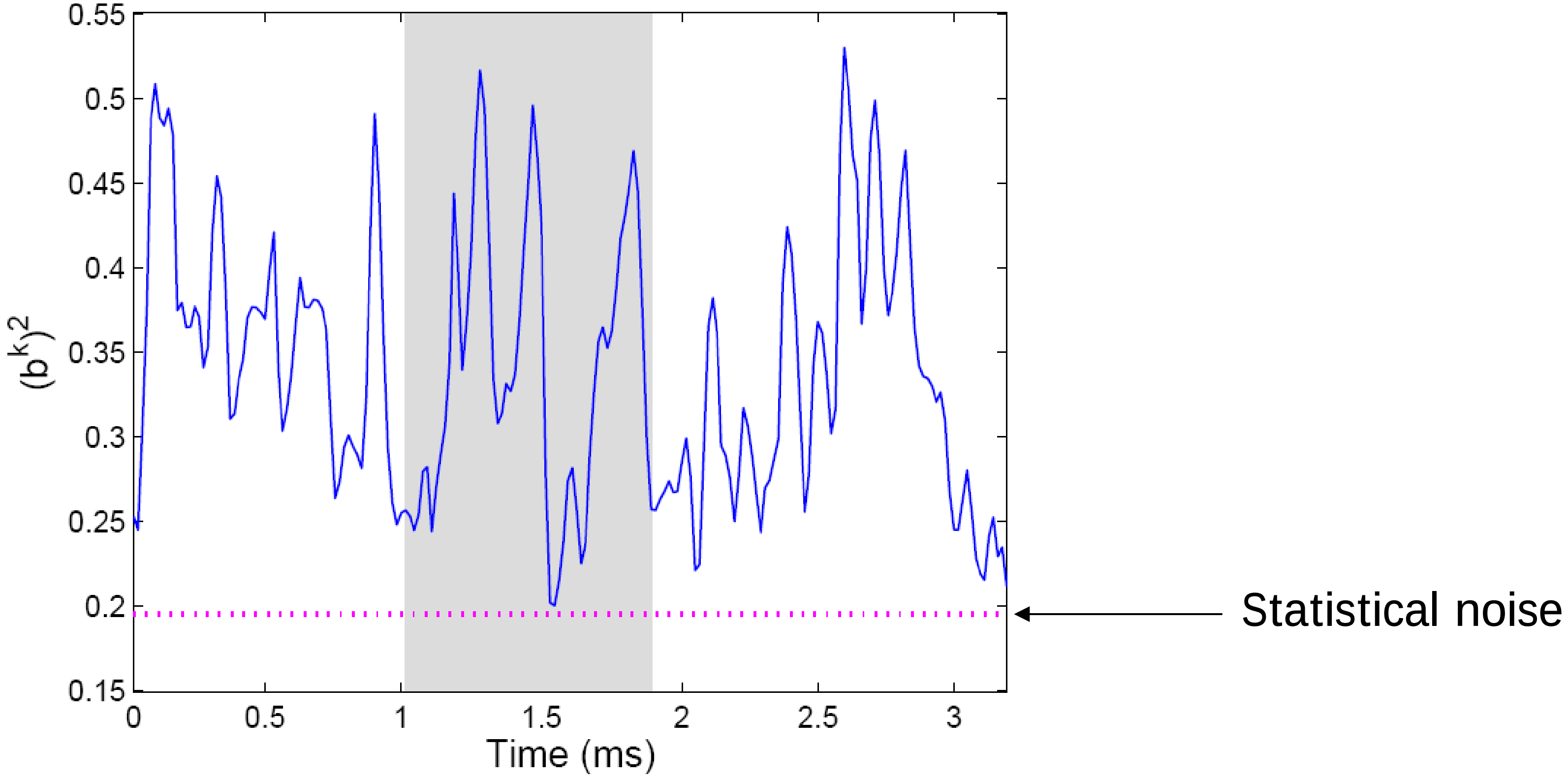

Results : dynamical analysis

Zooming a bicoherence burst: comparison spectrum/summed bicoherence => a m = 3 mode is created through mode coupling.

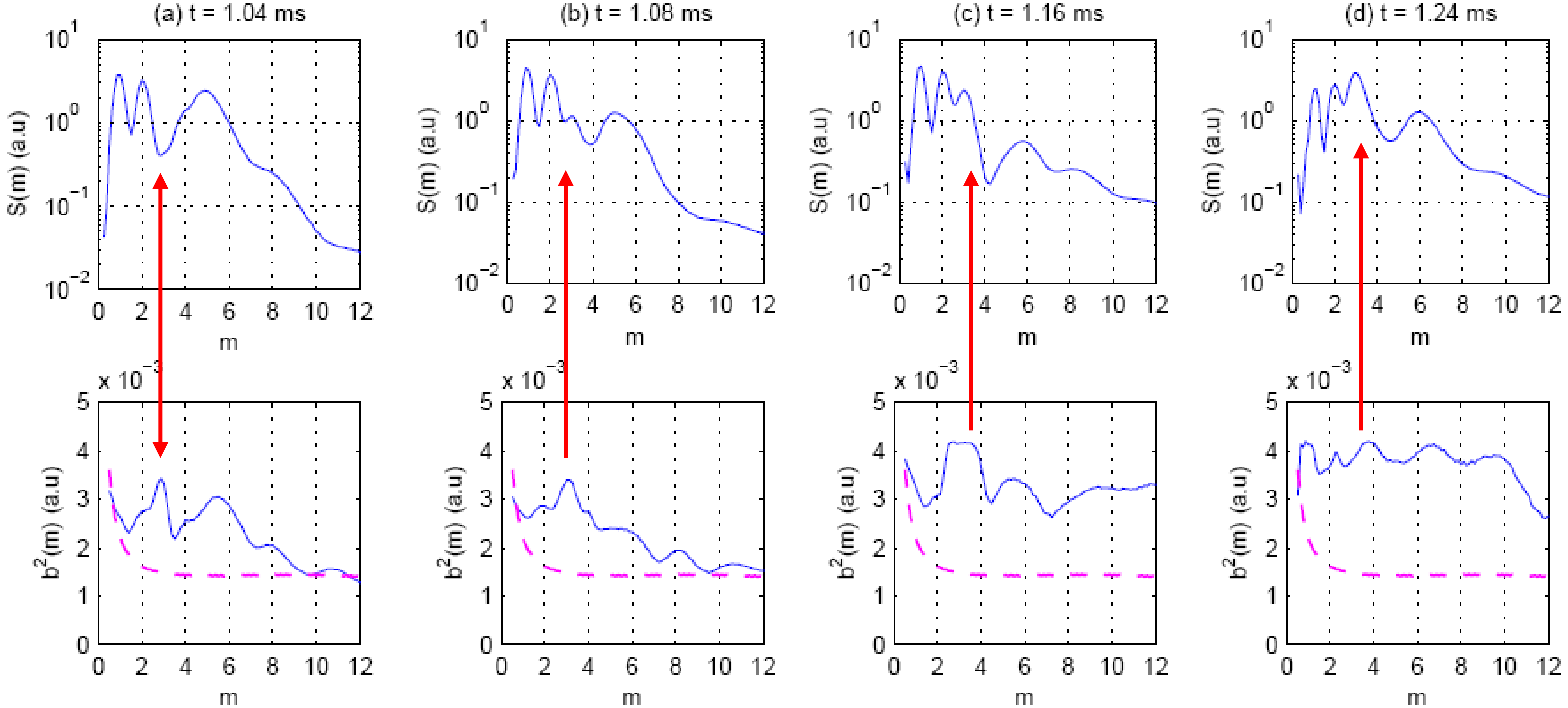

F. Brochard et al., Phys. Plasmas 13, 122305 (2006)

Experimental Setup: the MIRABELLE device

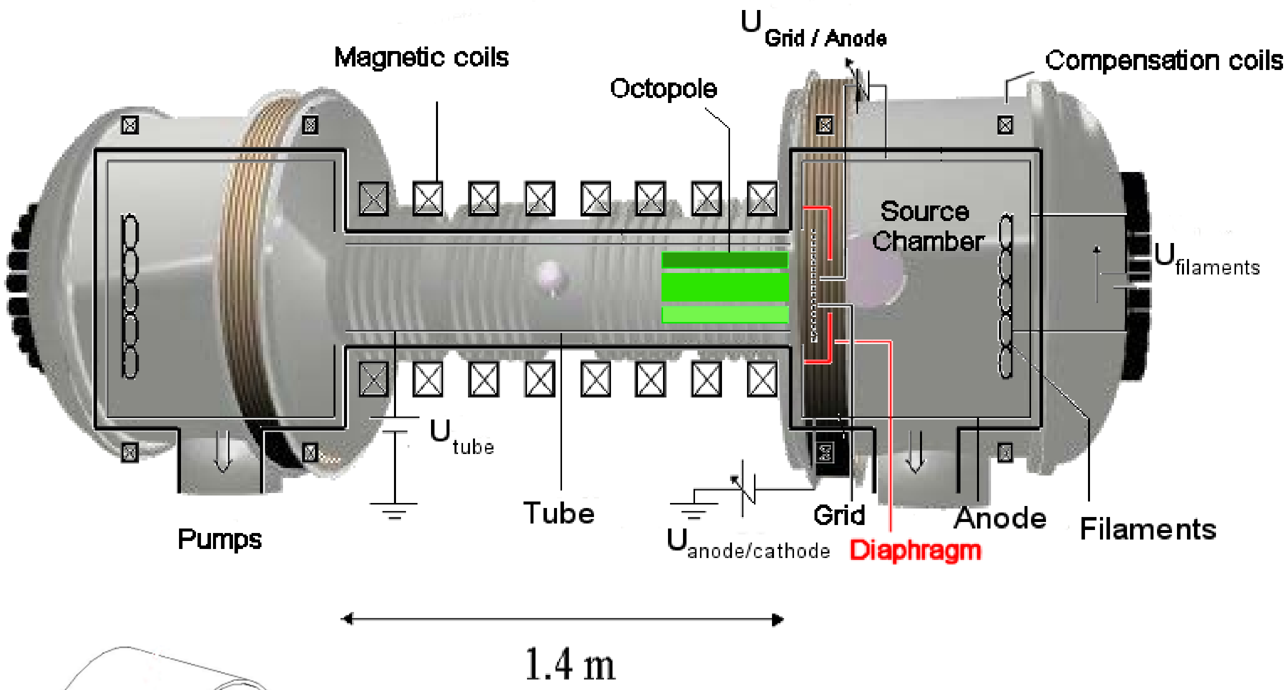

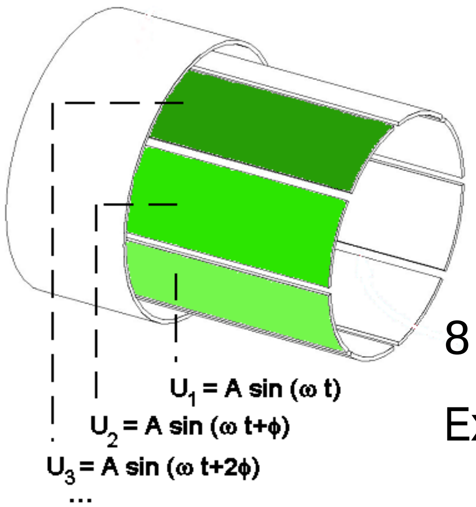

8 plates

Exciter

Plasma typical parameters:

- Argon plasma
- B = 0 – 130 mT
- P ~ 0.5-5 E^{-4} torrs
- Te ~ 1 – 3 eV , Ti ~ 0.02 eV
- $n_e \sim 10^{15} - 10^{16}\ m^{-3}$
- $\rho_S \sim 0.5 - 3$ cm

Spatiotemporal control of a weak turbulent state

The exciter plates are localised outside of the plasma ⇒ no limiter effect.

➢

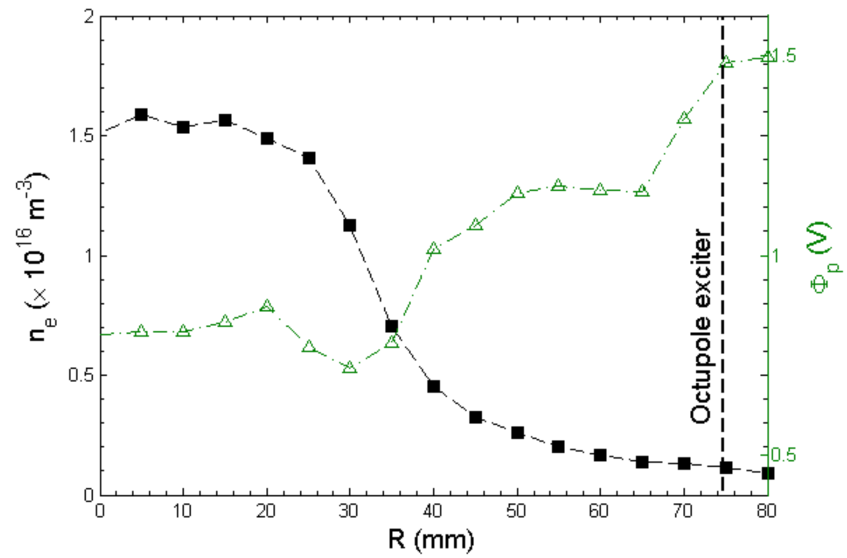

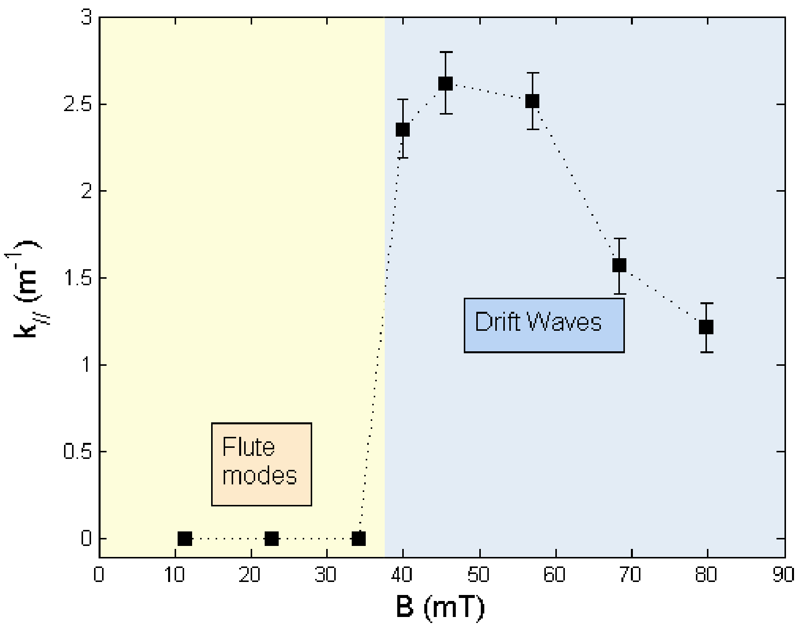

In Mirabelle, it is possible to select between "flute" modes (Kelvin-Helmholtz, Rayleigh-Taylor) at low field, and drift waves at high magnetic field.

F. Brochard et al., Phys. Plasmas 12, 062104 (2005).

Spatiotemporal control of a weak turbulent state

Example 1 : forcing of a m=1 Kelvin-Helmholtz mode

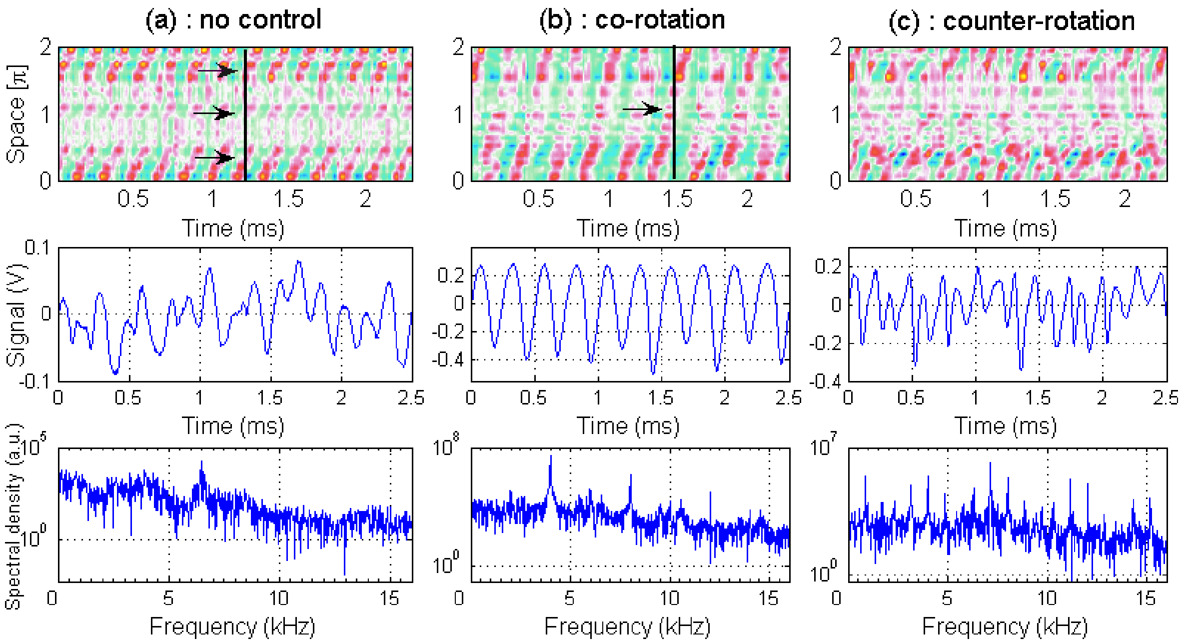

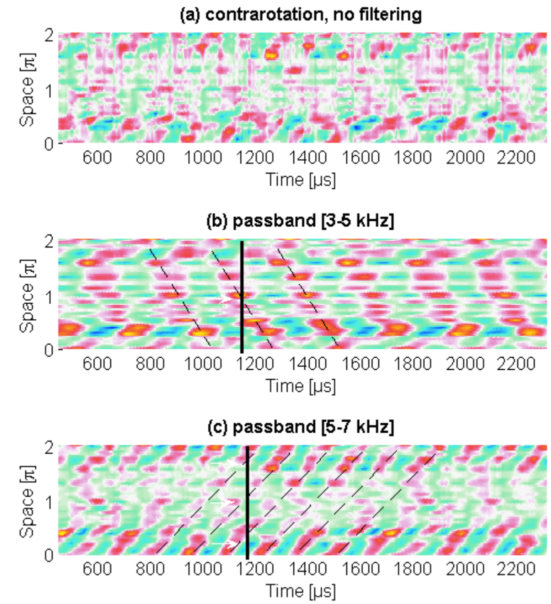

A m=1 mode at F_{ex}=4kHz is applied to a ~3 à 7 kHz irregular mode, for two rotation directions (amplitude 2V)

Filtering out the conter-rotation by using a 1st order band-pass filter

Spatiotemporal control of a weak turbulent state

- Spatiotemporal effect
- the m=3 mode is not totally suppressed.
- $k_{//}$=0 before and after control: same kind of mode.
- in the counter-rotation case, the applied spatiotemporal structure is simply superimposed. No coupling.

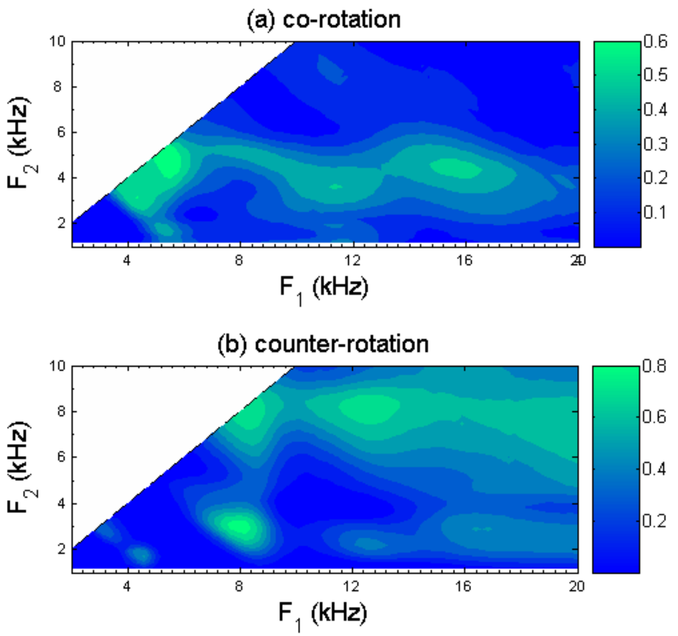

- Bicoherence analysis: coupling between F_{ex} and the instability only if co-rotation.

Bicoherence plot demonstrating the coupling between the forcing mode and plasma eigenmodes

F. Brochard et al., Phys. Plasmas 13, 052509 (2006).

Spatiotemporal control of a weak turbulent state

Ex.2 : synchronisation of a m=2 mode (Kelvin-Helmholtz)

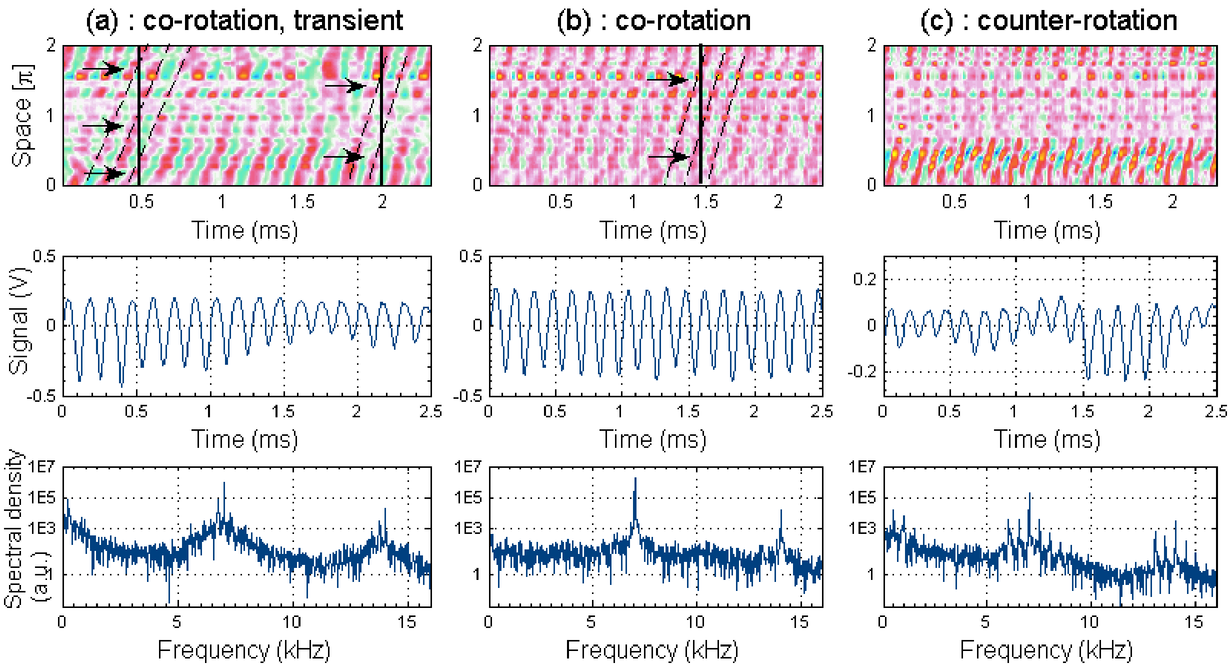

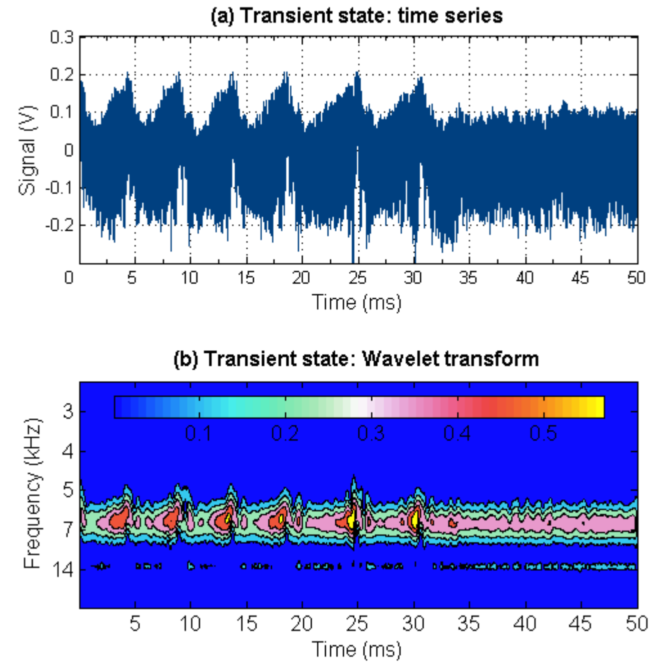

Forcing of a m=2 at F_{ex} = 7kHz on a m~3 at 7kHz (amplitude 1.2V)

Wavelet analysis showing the transition to the synchronized state

Driving a Turbulent state

The excitor can also be used to drive more turbulent states, through nonlinear wave-wave coupling leading to spectral enlargment (Ruelle-Takens scenario).

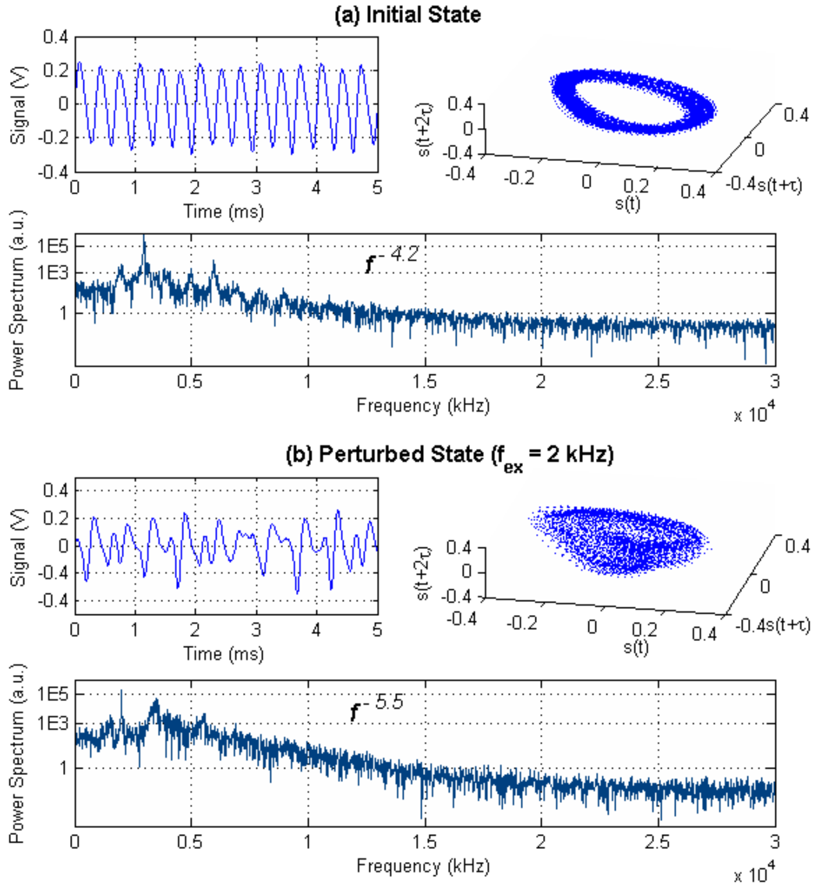

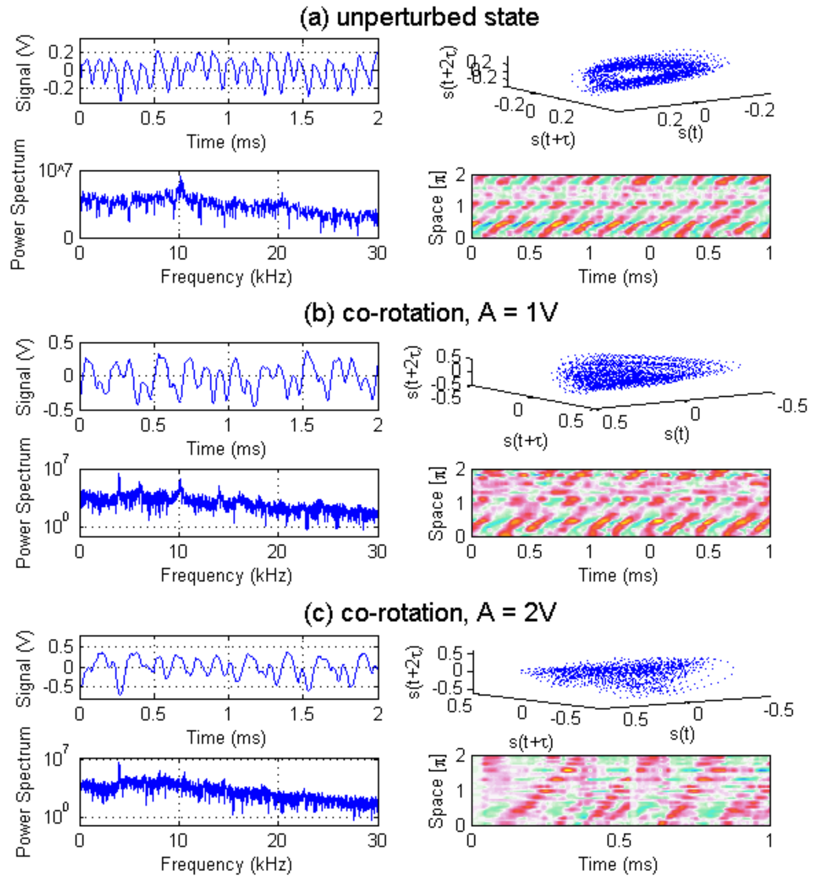

Generation of turbulence: Drift waves (left) and Kelvin-Helmholtz (right). The turbulence level depends on the amplitude of the applied signal on the exciter.

Fast camera data (test)

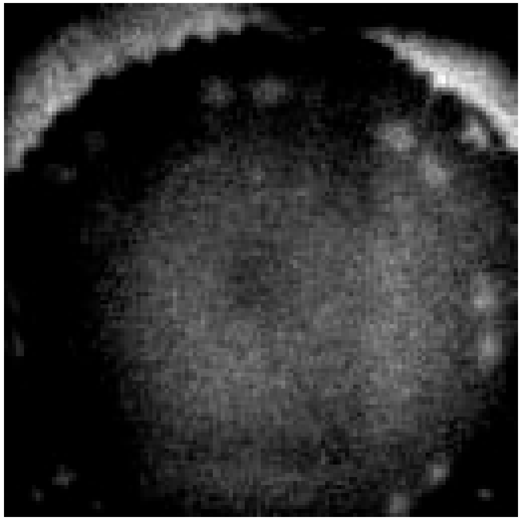

Raw data taken in the Mirabelle device

Drift wave, regular mode

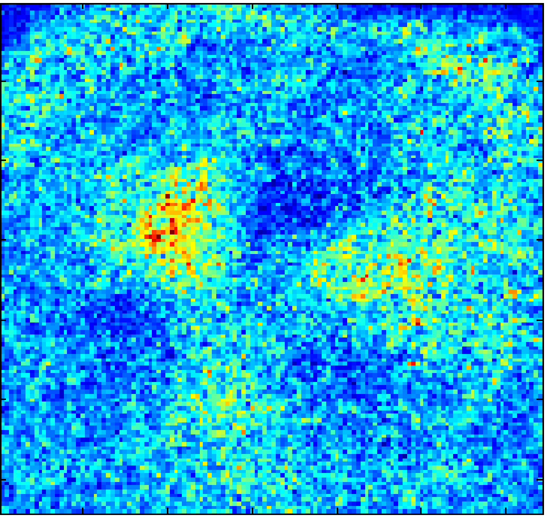

After substracting mean value at each pixel

After wavelet processing

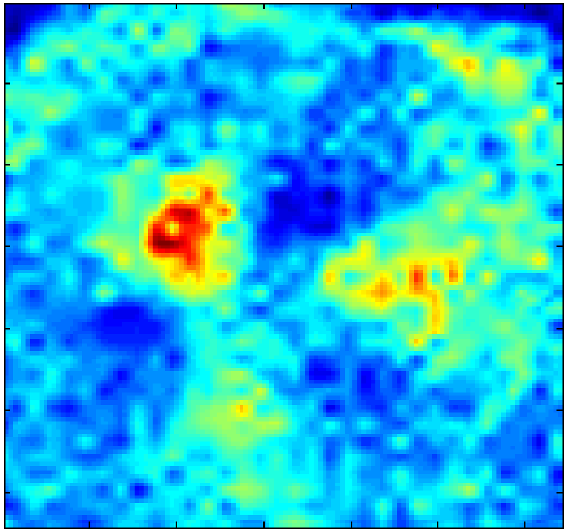

Conclusions and Perspectives

- Several methods are available
- The choice of the best method depends on the kind of information we want to extract from the data
- Fourier methods have many drawbacks when applied to non stationnary nonlinear signals
- Wavelets based tools are very useful, and especially to measure self-similiarity properties
- Among the last introduced methods the Hilbert-Huang transform has proven to be very efficient in filtering